

ACCEPTED VERSION

David J. Price, Nigel G. Bean, Joshua V. Ross, Jonathan Tuke
Designing group dose-response studies in the presence of transmission
Mathematical Biosciences, 2018; 304:62-78

© 2018 Elsevier Inc. All rights reserved.

This manuscript version is made available under the CC-BY-NC-ND 4.0 license
<http://creativecommons.org/licenses/by-nc-nd/4.0/>

Final publication at <http://dx.doi.org/10.1016/j.mbs.2018.07.007>

PERMISSIONS

<https://www.elsevier.com/about/our-business/policies/sharing>

Accepted Manuscript

Authors can share their accepted manuscript:

[12 months embargo]

After the embargo period

- via non-commercial hosting platforms such as their institutional repository
- via commercial sites with which Elsevier has an agreement

In all cases accepted manuscripts should:

- link to the formal publication via its DOI
- bear a CC-BY-NC-ND license – this is easy to do
- if aggregated with other manuscripts, for example in a repository or other site, be shared in alignment with our [hosting policy](#)
- not be added to or enhanced in any way to appear more like, or to substitute for, the published journal article

24 June 2020

<http://hdl.handle.net/2440/115562>

Designing group dose-response studies in the presence of transmission

David J. Price^{a,b}, Nigel G. Bean^{c,d}, Joshua V. Ross^{c,d}, Jonathan Tuke^{c,d}

^a*Centre for Epidemiology and Biostatistics, Melbourne School of Population and Global Health, The University of Melbourne, VIC 3010, Australia*

^b*Victorian Infectious Diseases Reference Laboratory Epidemiology Unit at The Peter Doherty Institute for Infection and Immunity, The University of Melbourne and Royal Melbourne Hospital, VIC 3000, Australia*

^c*School of Mathematical Sciences, University of Adelaide, SA 5005, Australia*

^d*ARC Centre of Excellence for Mathematical & Statistical Frontiers, School of Mathematical Sciences, University of Adelaide, SA 5005, Australia*

Abstract

Dose-response studies are used throughout pharmacology, toxicology and in clinical research to determine safe, effective, or hazardous doses of a substance. When involving animals, the subjects are often housed in groups; this is in fact mandatory in many countries for *social animals*, on ethical grounds. An issue that may consequently arise is that of unregulated between-subject dosing (transmission), where a subject may *transmit* the substance to another subject. Transmission will obviously impact the assessment of the dose-response relationship, and will lead to biases if not properly modelled. Here we present a method for determining the optimal design – pertaining to the size of groups, the doses, and the killing times – for such group dose-response experiments, in a Bayesian framework. Our results are of importance to minimising the number of animals required in order to accurately determine dose-response relationships. Furthermore, we additionally consider scenarios in which the estimation of the amount of transmission is also of interest. A particular motivating example is that of *Campylobacter jejuni* in chickens. Code is provided so that practitioners may determine the optimal design for their own studies.

Email address: david.j.price@alumni.adelaide.edu.au (David J. Price)

Keywords: Bayesian optimal experimental design, dose-response experiments, Markov chains, epidemic model.

1. Introduction

1 A group dose-response experiment involves exposing subjects to a range of doses
2 of a substance (for example, an infectious agent, or bacteria or a drug) and measuring
3 their responses (for example, if they became colonised) [2]. These experiments are
4 routinely used to characterise the relationship between the dose of a substance and
5 the response in a subject, known as the *dose-response relationship*.

6 Studies of this type have been widely used throughout pharmacology [27], toxi-
7 cology [3] and in clinical trials [1], and methods for characterising the dose-response
8 relationship developed [28]. However, a recent study by Conlan *et al.* noted a poten-
9 tial issue with such analyses when considering infectious agents [7]: in some cases,
10 subjects may *transmit* their dose to other subjects, hence complicating the analysis.
11 The motivating example is of *Campylobacter jejuni* in chickens.

12 The *Campylobacter* genus of bacteria is the most common cause of food-borne
13 diarrhoeal disease in developed and developing countries – surpassing *Salmonella* and
14 *Shigella* spp. [12]. Group dose-response experiments with *C. jejuni* in chickens are a
15 useful tool in understanding the dose-response and transmission characteristics of the
16 bacteria, allowing sensible measures to be put in place to contain, or eradicate, the
17 infection in livestock used for human consumption. Chickens are social animals, and
18 thus ethically are required to be co-housed [14]. Conlan *et al.* [7] noted that previous
19 statistical analyses of the dose-response characteristics of *C. jejuni* in chickens had
20 neglected the potential for transmission between co-housed subjects – resulting in
21 incorrect estimation of the dose-response relationship.

22 The presence of transmission in these experiments leads to an “all-or-nothing”
23 response if the subjects are observed too late – that is, once at least one subject
24 is infected within a group, transmission to the initially uninfected chickens leads to

25 more chickens being colonised than is representative of the administered dose. This
26 yields a lower estimated ID_{50} (i.e., the dose required to infect 50% of the population,
27 on average), and steeper slope-at-half-height – common statistics used to charac-
28 terise dose-response curves [7]. To limit between-subject dosing, one might attempt
29 to sample the chickens after a very short period of time following initial dosing.
30 However, there exists a latent period between a chicken being challenged and it be-
31 coming colonised (i.e., it presenting its response), thus this also provides inaccurate
32 assessment of the number of colonised subjects. Finally, a chicken is “observed” via
33 post-mortem caecal sampling, meaning that only one observation of each subject is
34 possible.

35 Studies of this form – grouped dose-response experiments with the potential for
36 between-subject dosing – are common, and given the ethical, financial and physical
37 constraints associated with such studies, determining their optimal experimental
38 design in order to obtain the most information about the dose-response relationship
39 is important. One must consider the allocation of the number of subjects to groups,
40 possibly different doses, and the associated time(s) to observe the process, in order to
41 gain the most information about the dose-response relationship. In particular, using
42 these optimal design tools, we can quantify the trade-off in information between
43 allocating many individuals to few groups (doses), or few individuals to many groups
44 (doses). We furthermore give consideration to scenarios in which the estimation of
45 the transmission rate is also of interest – highlighting the potential for these tools to
46 inform design of experiments where the purpose is understanding the transmission
47 dynamics of a pathogen (e.g., avian influenza as in [26]).

48 We work within a Bayesian framework, allowing for use of prior information
49 concerning the various components of the dose-response study, and transmission
50 dynamics. Our method involves a novel continuous-time Markov chain model for
51 the dynamics within such a study, combined with recently-developed methods for
52 Bayesian optimal experimental design [20, 21]. `MATLAB` code is provided so that

53 practitioners may determine the optimal design for their own studies.

54 **2. Methodology**

55 *2.1. Modelling of Group Dose-response Experiments*

56 The first step in determining the optimal experimental design for these exper-
57 iments is determining suitable models to represent the dynamics amongst a group
58 of subjects. In determining a suitable model, we must ensure we account for the
59 experimental aspects we wish to determine as part of our optimal designs. First and
60 foremost, we are interested in the optimal doses to allocate to subjects in order to
61 gain the most information about the dose-response relationship. Hence, we must
62 represent the dose-response relationships we believe are possible given the substance
63 and subjects being studied. This is achieved by specifying a suitable prior distribu-
64 tion for the model parameters, which results in a range of dose-response curves we
65 believe may eventuate from the experiment (examples given in Section 3).

66 We must also determine when to observe the process, to measure the response –
67 in this example, we count the number of infectious chickens in each group (i.e., our
68 data is the number of infectious individuals in each group). There are three impor-
69 tant considerations when determining the optimal observation time for these group
70 dose-response experiments. First, observation here is assumed to involve killing the
71 subject; hence, we have only one observation for each subject. Second, transmission
72 may occur which may in turn increase the number of colonised subjects we observe
73 for a given dose, thus skewing the dose-response relationship to appear steeper, and
74 reducing the estimate of the ID_{50} [7]. Hence, this suggests we should observe the
75 process early enough in order to mitigate transmission. However, the earlier ob-
76 servation time due to transmission is in direct competition with the third and final
77 consideration: the latent period. That is, there is a delay between exposure to a dose
78 (say via injection, or ingestion) and colonisation. Thus, in determining the optimal
79 observation time, we must allow sufficient time for the subject to pass through this

80 latent period, but still observe the process early enough to ensure that there has
 81 not been significant amounts of transmission between subjects. With regards to the
 82 design, we choose one dose and observation time for all chickens within a group –
 83 that is, each chicken within a group receives an identical dose, and is killed at the
 84 same time.

85 In order to cover these three important aspects – the dose-response relationship,
 86 a latent period, and transmission – we propose a continuous-time Markov chain
 87 model to incorporate each of these stages. We use the beta-Poisson model for the
 88 probability of infection, P_{inf} , for a subject given dose D . That is,

$$P_{\text{inf}}(D; \alpha, \delta) \approx 1 - \left(1 + \frac{D}{\delta}\right)^{-\alpha}. \quad (1)$$

This follows as the approximation to the hypergeometric model used by [7] – suitable
 when $\delta \gg \max(\alpha, 1)$. Common statistics used to characterise a dose-response
 relationship are the ID_{50} and the Slope-at-half-height (SHH). The ID_{50} represents
 the dose required to infect 50% of the population, and the slope-at-half-height is a
 measure of the susceptibility of the host to the pathogen [7]. The ID_{50} and SHH can
 be evaluated with respect to α and δ as follows:

$$\text{ID}_{50} = \delta(2^{1/\alpha} - 1), \quad \text{and,} \quad \text{SHH} = \frac{\log(10)}{2} \alpha \left(1 - \left(\frac{1}{2}\right)^{1/\alpha}\right).$$

89 Note that the slope-at-half-height is independent of δ .

90 The model we consider takes into account both the latent period of infection, as
 91 well as transmission between subjects. We propose a SE_kI Markov chain epidemic
 92 model, where: subjects begin the process as healthy; then, the subjects move into
 93 either the (first, of k) exposed class (with probability P_{inf} , i.e., they are colonised by
 94 the design dose), or the susceptible class (with probability $1 - P_{\text{inf}}$) otherwise. We
 95 choose to have more than one exposed class ($k > 1$) to allow the distribution of time
 96 spent in the latent period to follow an Erlang distribution – a more representative
 97 distribution of the latent period than the exponential distribution (e.g., [30, 23]).

98 Once a subject has passed through the k exposed classes, they transition into the
 99 infectious class. Once a subject is in the infectious class, they may transmit some
 100 dose to uncolonised subjects, where β is the effective transmission rate. Figure
 101 1 provides a graphical representation of this process. In the example considered
 102 herein, we use $k = 2$ and $\gamma = 2$, in order to achieve a mean time between exposure
 103 and infectiousness of 1 day (and probability 0.9 of being infectious by day 2) [5],
 104 consistent with values reported in [6] on data from [29].

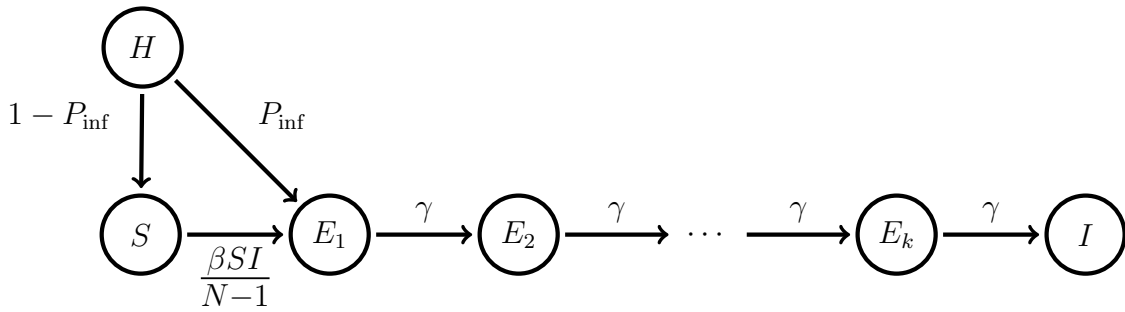


Figure 1: Diagram illustrating the progression of subjects through the complete model. Subjects begin as Healthy (H), and after being dosed, move to the first Exposed class (E_1) with probability P_{inf} , or otherwise they move to the Susceptible class (S). Once exposed, the subjects pass through k exposed classes (E_1, \dots, E_k), each at rate γ , to reach the Infectious class (I). Once in the infectious class, the subject can transmit the infection to subjects in the susceptible class with effective transmission rate β .

Note that we need to keep track of all but one of the compartments, as we have a fixed population size, N ; hence, the state corresponding to the infectious class is omitted from our state space and rate description. We define the transition rates for the SE_kI Markov chain model on the state space,

$$\mathcal{S} = \{(s, e_1, \dots, e_k) : 0 \leq s, e_1, \dots, e_k, s + e_1 + \dots + e_k \leq N\}$$

as follows:

$$\begin{aligned}
q_{(s,e_1,\dots,e_k),(s-1,e_1+1,\dots,e_k)} &= \beta \frac{s(N-s-\sum_{l=1}^k e_l)}{N-1}, \\
q_{(s,\dots,e_j,e_{j+1},\dots),(s,\dots,e_{j-1},e_{j+1}+1,\dots)} &= \gamma e_j, \quad \text{for } j = 1, \dots, k-1, \\
q_{(s,\dots,e_k),(s,\dots,e_k-1)} &= \gamma e_k.
\end{aligned}$$

An individual subject begins as ‘exposed’ with probability P_{inf} . Hence, the probability of having m initially exposed subjects follows a binomial distribution with N trials, and probability of success $P_{\text{inf}}(D; \alpha, \delta)$. That is, the initial state of our process is given by,

$$P(s = N - m, e_1 = m, e_j = 0, \text{ for } j = 2, \dots, k) = \binom{N}{m} P_{\text{inf}}^m (1 - P_{\text{inf}})^{N-m}.$$

105 The Markov chain model is then initiated from the state $\{s = N - m, e_1 = m, e_2 =$
106 $0, \dots, e_k = 0\}$. We assume that subjects can only be identified as colonised once
107 they enter the infectious class, which is an important assumption when it comes to
108 determining the optimal observation times later.

109 2.2. Background: Optimal Experimental Design

110 The aim of optimal experimental design is to determine the best experimental
111 setup in order to maximise some utility of the experiment. To achieve this aim, we
112 specify a utility function $U(\boldsymbol{\theta}, \mathbf{x}, d)$, where d is an experimental design chosen from
113 the set of all designs \mathcal{D} , $\boldsymbol{\theta}$ is the model parameters and \mathbf{x} is the data. This utility
114 function represents how we ‘value’ a design. We are interested in the expected utility
115 of using design d , over the unknown model parameters and data. That is, we wish
116 to evaluate the following,

$$u(d) = E_{\boldsymbol{\theta}, \mathbf{x}}[U(\boldsymbol{\theta}, \mathbf{x}, d)] = \int_{\mathbf{x}} \int_{\boldsymbol{\theta}} U(\boldsymbol{\theta}, \mathbf{x}, d) p(\mathbf{x} | \boldsymbol{\theta}, d) p(\boldsymbol{\theta}) d\boldsymbol{\theta} d\mathbf{x}, \quad (2)$$

where $p(\mathbf{x} | \boldsymbol{\theta}, d)$ is the likelihood function of the unobserved data, under design d , and $p(\boldsymbol{\theta})$ is the prior distribution of the model parameters. The optimal design d^*

maximises the expected utility over the design space \mathcal{D} ,

$$d^* = \operatorname{argmax}_{d \in \mathcal{D}} u(d).$$

117 The utility function is chosen to represent those aspects of the experiment deemed
 118 to be of importance. See [4] and [25] for a review of Bayesian optimal experimental
 119 design.

120 2.3. Choice of Utility

121 In this work, we investigate two utility functions with the purpose of parameter
 122 estimation, namely the Kullback-Leibler divergence (KLD), and the Mean Absolute
 123 Percentage Error (MAPE) of a point estimate from the posterior distribution (here,
 124 we use the posterior median).

125 The Kullback-Leibler divergence is given by:

$$U(\mathbf{x}, d) = \int_{\boldsymbol{\theta}} \log \left(\frac{p(\boldsymbol{\theta} \mid \mathbf{x}, d)}{p(\boldsymbol{\theta})} \right) p(\boldsymbol{\theta} \mid \mathbf{x}, d) d\boldsymbol{\theta}, \quad (3)$$

126 where $p(\boldsymbol{\theta} \mid \mathbf{x}, d)$ is the posterior distribution having observed data \mathbf{x} at design
 127 d . The Kullback-Leibler divergence is the most commonly used utility function
 128 when the purpose of the experiment is parameter estimation (e.g., [8], [15], [10],
 129 [24], [19], [20]). This is perhaps due to its independence to model parameterisation,
 130 or the convenient interpretation: designs which maximise the EKLD maximise the
 131 increase in information between the prior and the posterior distributions, which can
 132 be interpreted as maximising the amount *learned* from the experiment. However, of
 133 concern is the potential for this utility to select designs that maximise the divergence
 134 as a consequence of biases in the likelihood that are more likely, or stronger, for those
 135 particular designs. As an alternative, we propose the following utility with the aim
 136 of estimating model parameters accurately.

137 The Mean Absolute Percentage Error (MAPE) for true (known) parameters $\boldsymbol{\theta} =$
 138 $(\theta_1, \theta_2, \dots, \theta_p)$ and estimated parameters $\hat{\boldsymbol{\theta}} = (\hat{\theta}_1, \hat{\theta}_2, \dots, \hat{\theta}_p)$ is given by:

$$U(\mathbf{x}, d) = \frac{1}{p} \sum_{j=1}^p \frac{|\theta_j - \hat{\theta}_j|}{\theta_j}, \quad (4)$$

139 where we choose as our parameter estimates $\hat{\boldsymbol{\theta}}$ the median *a posteriori* estimate from
 140 the posterior distribution $p(\boldsymbol{\theta} \mid \mathbf{x}, d)$. We choose the median over the mode, as evalu-
 141 ating the mode of a high-dimensional distribution can be computationally inefficient
 142 and cumbersome (e.g., [10]). In this work, we are only considering experimental
 143 design for the purpose of parameter estimation, where it is assumed that the model
 144 is known. One could include model uncertainty in this process, or, if the purpose
 145 was to best discriminate between a number of competing models, alternative utility
 146 functions exist for this purpose (e.g., [9]).

147 Unfortunately, analytic evaluation of the expected utility function $u(d)$ can rarely
 148 be achieved. Hence, we evaluate approximations to equations 3 and 4, and hence the
 149 expected utility for each design in equation 2, using the following algorithm [20].

150 2.4. Evaluation of Utility: The ABCdE Algorithm

151 To evaluate the utility, we take the approach used within the ABCdE algorithm of
 152 [20], which has proven beneficial for this type of discrete data problem. The method
 153 utilises an Approximate Bayesian Computation (ABC) approach to approximating
 154 the posterior distribution, which relies on simulations of the model (e.g., [16]).

155 Note that the data in this example are the number of infectious individuals in each
 156 group, e.g., $\mathbf{x}_j = (i_{1j}, i_{2j}, \dots)$, where i_{kj} is the number of infectious individuals in
 157 the j^{th} simulation of the k^{th} group for a given design. We provide a brief description
 158 below, but direct the reader to the original manuscript for full details.

159 For each design, we use each set of the pre-simulated data as the “observed
 160 datum” one-by-one, and evaluate the utility using all the N_{pre} data as “simulated
 161 data”. This creates a set of posterior samples having observed every set of simulated
 162 data for a particular design. That is, for simulated data $\mathbf{x}_1, \mathbf{x}_2, \dots, \mathbf{x}_{N_{pre}}$ under
 163 design d , we determine ABC posteriors $[\hat{p}(\boldsymbol{\theta} \mid \mathbf{x}_1, d), \hat{p}(\boldsymbol{\theta} \mid \mathbf{x}_2, d), \dots, \hat{p}(\boldsymbol{\theta} \mid \mathbf{x}_{N_{pre}}, d)]$
 164 using Algorithm 1 (Appendix 6.1). For the current design, we pre-simulate all N_{pre}
 165 simulated data sets corresponding to sampled parameter values, and thus we can

166 pass pre-simulated data and corresponding parameter values to Algorithm 1 to form
 167 the posterior distributions.

168 We evaluate the utility using each of these N_{pre} posterior distributions under a
 169 particular design, and take the average of these N_{pre} values to be our estimate of
 170 the expected utility for that design. The optimal design is then the design that
 171 returns the largest expected utility. The full algorithm is outlined in Appendix 6.1
 172 (Algorithm 2). We propose that the number of simulations N_{pre} and ABC tolerance
 173 ϵ be chosen in the same way as one would choose the number of simulations and
 174 tolerance when using ABC for inference (see, for example, [18]).

175 For gridded parameter values $\boldsymbol{\theta}_1, \boldsymbol{\theta}_2, \dots, \boldsymbol{\theta}_l$ (allocated prior to running the algo-
 176 rithm, and fixed for all designs), we evaluate a Monte-Carlo approximation to the
 177 Expected Kullback-Leibler divergence (EKLD) as:

$$u(d) = \frac{1}{N_{pre}} \sum_{i=1}^{N_{pre}} \sum_{j=1}^l \log \left(\frac{p(\boldsymbol{\theta}_j | \mathbf{x}_i, d)}{p(\boldsymbol{\theta}_j)} \right) p(\boldsymbol{\theta}_j | \mathbf{x}_i, d). \quad (5)$$

178 Similarly, the average MAPE for design d , where the i^{th} simulation ($i = 1, \dots, N_{pre}$),
 179 $\mathbf{x}_i \sim p((\theta_{i1}, \dots, \theta_{ip}))$, has median *a posteriori* $\hat{\boldsymbol{\theta}}_i = (\hat{\theta}_{i1}, \dots, \hat{\theta}_{ip})$, is estimated by:

$$u(d) = \frac{1}{p \times N_{pre}} \sum_{i=1}^{N_{pre}} \sum_{j=1}^p \frac{|\theta_{ij} - \hat{\theta}_{ij}|}{\theta_{ij}}. \quad (6)$$

180 Note that inference under a particular design will be identical for the same set
 181 of observed data. For this reason, when dealing with discrete data, we evaluate a
 182 posterior distribution corresponding to each *unique* data set and use this distribution
 183 when evaluating (5) and (6). The frequency of that set of observed datum under the
 184 current design is then used to weight the contribution to the expected utility.

185 2.5. Design Search: The INSH Algorithm

186 The optimisation routine to find the optimal designs is detailed in [21], however
 187 we provide a brief description here.

188 The Induced Natural Selection Heuristic (INSH) is an optimisation heuristic to
189 efficiently search across a high-dimensional design space and find (near-) optimal
190 designs. At each iteration of the algorithm we consider a number of designs, and
191 through some mechanism, we retain some designs (e.g., top $\rho\%$, or best r designs)
192 – thus, inducing selection. Each of the retained designs then populate the next it-
193 eration of the algorithm by sampling m designs around each of them from some
194 distribution. By not combining the accepted samples at each iteration, we are able
195 to efficiently explore multiple regions of the design space simultaneously. Parallel-
196 computing is used to efficiently generate the data and evaluate the utility of each
197 design at each iteration. The initial designs used to start the algorithm can be
198 allocated across a grid, or randomly selected over the design space (e.g., via latin
199 hypercube sampling). Here, prior information regarding regions of the design space
200 with high-utility can be incorporated to allocate these initial designs. The algorithm
201 is outlined in Appendix 6.1 (Algorithm 3). Choices of each component of the algo-
202 rithm (i.e., initial designs, acceptance criteria, sampling distribution and stopping
203 criteria), are detailed in Section 3.

204 2.6. Case Study

205 Of particular interest in this paper are group dose-response challenge experiments
206 to monitor the spread of the bacteria *Campylobacter jejuni* amongst chickens. *C.*
207 *jejuni* is zoonotic, meaning it spreads from animals to humans, and is a common cause
208 of intestinal disease in humans [22]. Incidence of *C. jejuni* infection amongst humans
209 could be dramatically reduced through the prevention of food-borne transmission
210 [31]. Thus, a solid understanding of the dynamics of the bacteria through a flock of
211 chickens, which are to be used for human consumption, is paramount.

212 2.7. Prior Distributions

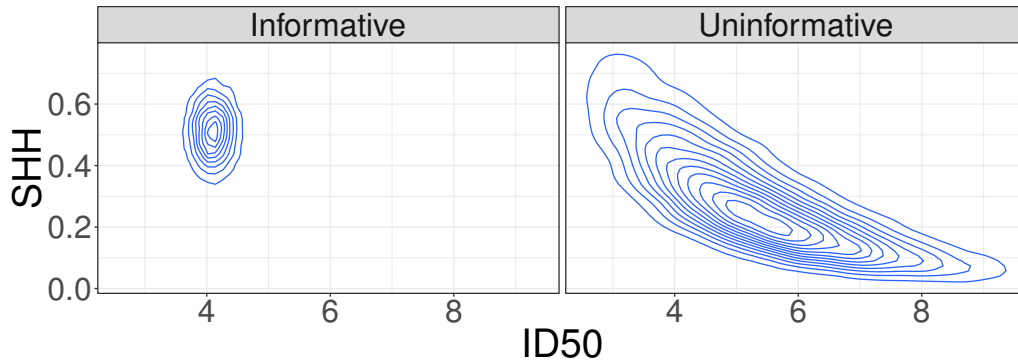
213 In the following examples, we consider two scenarios: 1) where we have a reason-
214 ably informative prior distribution, and 2) where we have a relatively uninformative

215 prior distribution. In order to more closely represent a practical example, we place
216 prior distributions on the ID_{50} and SHH, rather than α and δ in the dose-response
217 model. In order to motivate the prior distributions for the ID_{50} and SHH in these
218 examples, we use the estimated distributions of the 2- and 14-day old chicks re-
219 ported in [7] (specifically, Fig 3a on page 8) – in particular, the prior distributions
220 in the informative scenario represent the estimated distributions for the 2-day old
221 chicks, whereas the prior distributions specified in the uninformative scenario span
222 the reported distributions of both the 2- and 14-day old chicks.

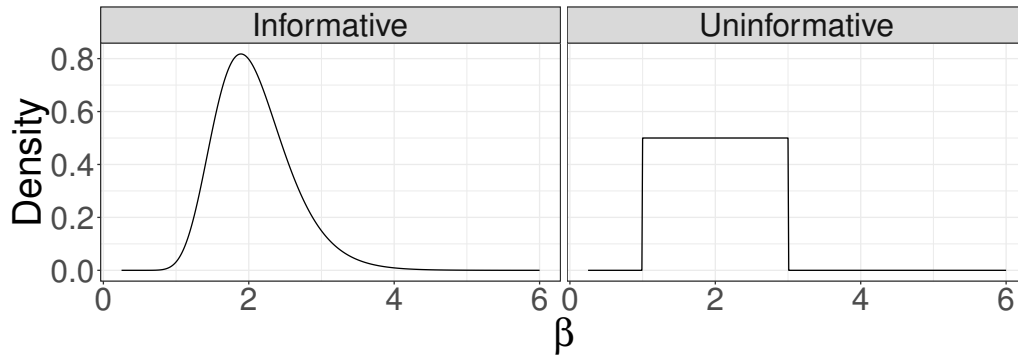
223 In the informative scenario, we place independent normal prior distributions on
224 each of the ID_{50} and SHH – $N(4.10, 0.225)$, and $N(0.51, 0.08)$, respectively – and a
225 $\log - N(0.7, 0.25)$ prior distribution on β . In the uninformative scenario, we induce
226 a correlation between the two parameters through a multivariate normal copula,
227 such that the marginal prior distributions of ID_{50} and SHH are $\text{Gamma}(14.5, 0.35)$
228 and $\text{Gamma}(12, 0.025)$, respectively, with a correlation of -0.85. The uninformative
229 prior distribution for β is $U(1, 3)$. When sampling from the prior, lower limits were
230 specified to ensure positive values were sampled, and an upper limit on the slope-
231 at-half-height was enforced at $(1/2)\log(10)\log(2)$, so as to not violate the hypothesis
232 of independent action [7]. The resulting prior distributions for the two scenarios
233 are shown in Figure 2. The experimental design method and all inference examples
234 herein, are with respect to the ID_{50} , SHH, and transmission rate β (where applicable).

235 *2.8. Design Space*

236 Consider a scenario where we are limited by resources – e.g., a fixed number
237 of chickens, doses or maximum time over which we may conduct the experiment.
238 Specifically, assume we are able to dose at most $N = 40$ chickens. We are interested
239 in determining optimal Bayesian experimental designs with respect to the number
240 of groups to allocate the fixed number of subjects to, the dose to allocate to each
241 group, and the time to sample each group. The ranges of these design parameters are
242 presented in Table 1. Note, we are dealing with a social animal, and as such, subjects



(a) Prior distributions on ID_{50} and Slope-at-half-height (SHH) under both the informative and uninformative scenarios.



(b) Prior distributions on transmission rate, β , under both the informative and uninformative scenarios

Figure 2: Prior distributions for ID_{50} , SHH and β in the informative and uninformative scenarios described above.

243 must be co-housed. That is, we assume that the chickens are allocated amongst at
 244 most five groups. Due to limitations by which one can generate a dose of infectious
 245 bacteria (e.g., growing colonies, dilution, etc.), we consider doses in step sizes of
 246 $0.5 \log_{10}CFU$ as practically feasible [13]. However, we note that improvements in
 247 microfluidics technology will lead to the ability to produce more precise inocula in
 248 the future [13], and so we also present results on a finer grid in the Supplementary
 249 Material.

Table 1: Typical values of design parameters considered when determining the optimal experimental designs.

| Design aspect | Typical Values |
|---------------------------|---|
| Number of groups (G) | $\{2,3,4,5\}$ |
| Dose allocation (A) | $\{0.5,1.00,1.50,\dots,10.00\}$ \log_{10} CFU |
| Observation times (T) | $\{0.05,0.10,0.15,\dots,6.00\}$ days |

250 We consider only the number of groups G , rather than the number of groups
 251 and the number of chickens in each group – specifically, we assume that the $N = 40$
 252 chickens are to be divided evenly among two, three, four or five groups (that is, 20,
 253 13, 10 or 8 chickens per group). Note that throughout we refer to the dose in units
 254 of \log_{10} colony forming units (CFU), i.e., we refer to a dose of 10^4 CFU, as a dose
 255 of 4. We allow any number of groups to receive the same dose, and each group can
 256 have a different observation time – however, each individual within a group has the
 257 same dose and observation time.

258 We note that the Bayesian optimal designs are specific to the prior distributions
 259 chosen; hence, the results we provide are not comprehensive. We will provide dis-
 260 cussion, where appropriate, to the sensitivity of the optimal designs to the choice
 261 of prior distributions, and provide `MATLAB` code for individuals to determine optimal
 262 designs for their own experiments.

263 3. Results

264 Recall, we consider two scenarios: 1) where we have an informative prior dis-
 265 tribution on the model parameters, and 2) where we have an uninformative prior
 266 distribution. For both scenarios, we consider the optimal designs with respect to
 267 both 1) the EKLD, and 2) the MAPE. Furthermore, we also establish the optimal
 268 designs when we are interested in either 1) the dose-response parameters only, 2)

269 the dose-response and the transmission rate parameter, and 3) the transmission rate
270 parameter only. That is, in total, we consider 12 different sets of results. We present
271 the optimal designs obtained via the INSH algorithm, in each example, and provide
272 figures demonstrating the regions (with respect to the dose and observation time)
273 that each group should be allocated to – akin to sampling windows considered in
274 pharmacokinetic experiments (e.g., [11], [17], [21]). We describe these regions by
275 taking the “top” designs from the INSH algorithm output, and drawing a convex
276 hull around each group – here, we consider the top 0.05% of designs considered by
277 INSH, ranked by their utility (corresponding to approximately 135 designs).

278 We demonstrate how well each design performs with regards to inference for all
279 parameters. In particular, for 200 simulated experiments, we evaluate the bias (of
280 the posterior median estimate) and variance of the posterior distributions evaluated
281 under each design for each simulated experiment. The posterior distributions were
282 evaluated using a standard ABC-rejection algorithm (Algorithm 1 in Appendix 6.1)
283 with 2,000,000 simulations, and a tolerance of $\epsilon = 0.25 \times G$. Figures illustrating the
284 convergence of the INSH algorithm – with respect to the number of designs of each
285 group size being considered, and the utility of all designs under consideration at each
286 wave – for each scenario are presented in Appendix 6.3.

287 *3.1. Optimal Designs from the INSH Algorithm*

288 For this problem, we have a number of different choices for the INSH algorithm.
289 In particular, the allocation of the initial designs, the acceptance criteria, the per-
290 turbation kernel (to sample new designs), and the stopping criteria. Steps 3-10 of
291 Algorithm 2 (ABCdE) are used to evaluate the utility for each design, as this ap-
292 proach has proven efficient for discrete data sets as we consider here. We allocate the
293 initial designs according to a uniform distribution across the range of the design vari-
294 ables (given in Table 1), for each number of groups ($G = 2, 3, 4, 5$). We specify the
295 number of initial designs for each group size according to our belief about the location
296 of the optimal design, and the size of the design space within each group size. In each

297 example considered herein, we begin with 50, 100, 150, 500 designs for $G = 2, 3, 4, 5$,
 298 respectively (a total of 800 designs in the first iteration). At each iteration, we ac-
 299 cept the best $r_w = (150, 75, 30)$ designs, and sample $m_w = (3, 6, 15)$ new designs
 300 around each accepted design (thus, considering 450 designs at each iteration), for 30,
 301 15 and 15 iterations each (i.e., first 30 iterations are exploring the space, accepting
 302 the best 150 designs and sampling three new designs around each accepted design).
 303 New designs are sampled according to a truncated-multivariate normal distribution
 304 (truncated to the limits of the design space), centred on the retained designs, with
 305 standard deviation for the dose allocation (A), $\sigma_w^A = (1.0, 0.75, 0.5)$ and observation
 306 time (T), $\sigma_w^T = (0.1, 0.075, 0.05)$, for 30, 15 and 15 iterations, as above. The updat-
 307 ing of r , m , σ^A and σ^T across each iteration is done in order to reduce exploration
 308 and increase exploitation, as the algorithm progresses. Table 2 contains the resulting
 309 optimal experimental design for each scenario.

310 Figures 3 and 4 show the dose and time combination for each group of the designs
 311 (i.e., the coloured groups $1, \dots, G$ represent the G groups in the design). The figures
 312 show convex hulls around the top designs with respect to the EKLD and MAPE
 313 (respectively). The designs have been jittered slightly so that one can identify where
 314 more design points for each group are clustered.

| Scenario | Utility | Target Parameters | G | Optimal Design: A: Dose (\log_{10} CFU); T: Obs. Time (days) |
|----------|---------|-------------------------|---|--|
| 1 | EKLD | (ID_{50}, SHH) | 5 | $A = (0.50, 1.00, 1.50, 2.00, 9.00)$ $T = (1.30, 1.30, 1.15, 1.05, 0.90)$ |
| 1 | MAPE | (ID_{50}, SHH) | 2 | $A = (1.50, 2.00)$ $T = (1.95, 1.90)$ |
| 1 | EKLD | (ID_{50}, SHH, β) | 5 | $A = (0.50, 1.00, 2.50, 5.50, 6.00)$ $T = (1.45, 1.30, 0.75, 0.85, 0.85)$ |
| 1 | MAPE | (ID_{50}, SHH, β) | 2 | $A = (0.50, 1.00)$ $T = (4.20, 3.70)$ |
| 1 | EKLD | (β) | 5 | $A = (0.50, 1.00, 1.50, 3.00, 8.50)$ $T = (1.40, 1.30, 0.95, 0.90, 0.85)$ |
| 1 | MAPE | (β) | 2 | $A = (2.40, 2.45)$ $T = (5.00, 4.90)$ |
| 2 | EKLD | (ID_{50}, SHH) | 5 | $A = (0.50, 1.00, 1.50, 3.00, 7.50)$ $T = (1.35, 1.45, 1.50, 0.90, 0.90)$ |
| 2 | MAPE | (ID_{50}, SHH) | 2 | $A = (2.00, 2.50)$ $T = (1.75, 1.80)$ |
| 2 | EKLD | (ID_{50}, SHH, β) | 5 | $A = (0.50, 1.00, 1.50, 2.50, 5.00)$ $T = (1.45, 1.55, 1.05, 0.95, 0.95)$ |
| 2 | MAPE | (ID_{50}, SHH, β) | 2 | $A = (0.50, 2.50)$ $T = (4.45, 2.05)$ |
| 2 | EKLD | (β) | 5 | $A = (0.50, 1.00, 1.50, 2.50, 9.00)$ $T = (1.40, 1.45, 0.95, 0.85, 0.85)$ |
| 2 | MAPE | (β) | 2 | $A = (0.50, 1.00)$ $T = (4.15, 4.05)$ |

Table 2: Optimal designs corresponding to two different scenarios ((1) informative and (2) uninformative prior distributions), according to two different utility functions (EKLD and MAPE), where the parameters of interest are either just the dose-response parameters (ID_{50}, SHH) , both the dose-response and transmission rate parameters (ID_{50}, SHH, β) , or the transmission parameter (β) .

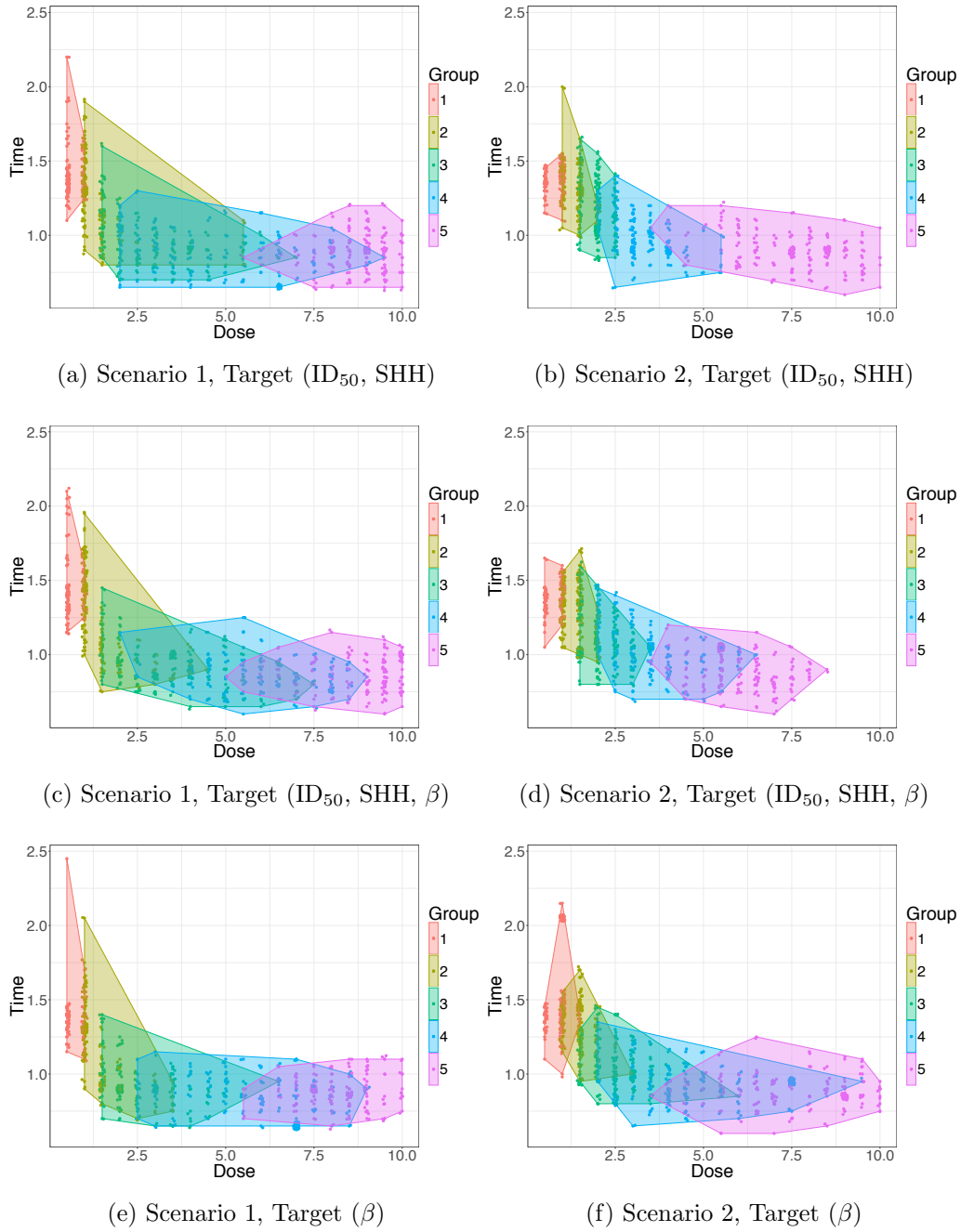


Figure 3: Convex hull plots demonstrating the dose-time pairing for each group, for the best 0.05% of designs according to the EKLD from the INSH algorithm, for Scenarios 1 and 2, when targeting each of (ID_{50}, SHH) , (ID_{50}, SHH, β) , and (β) .

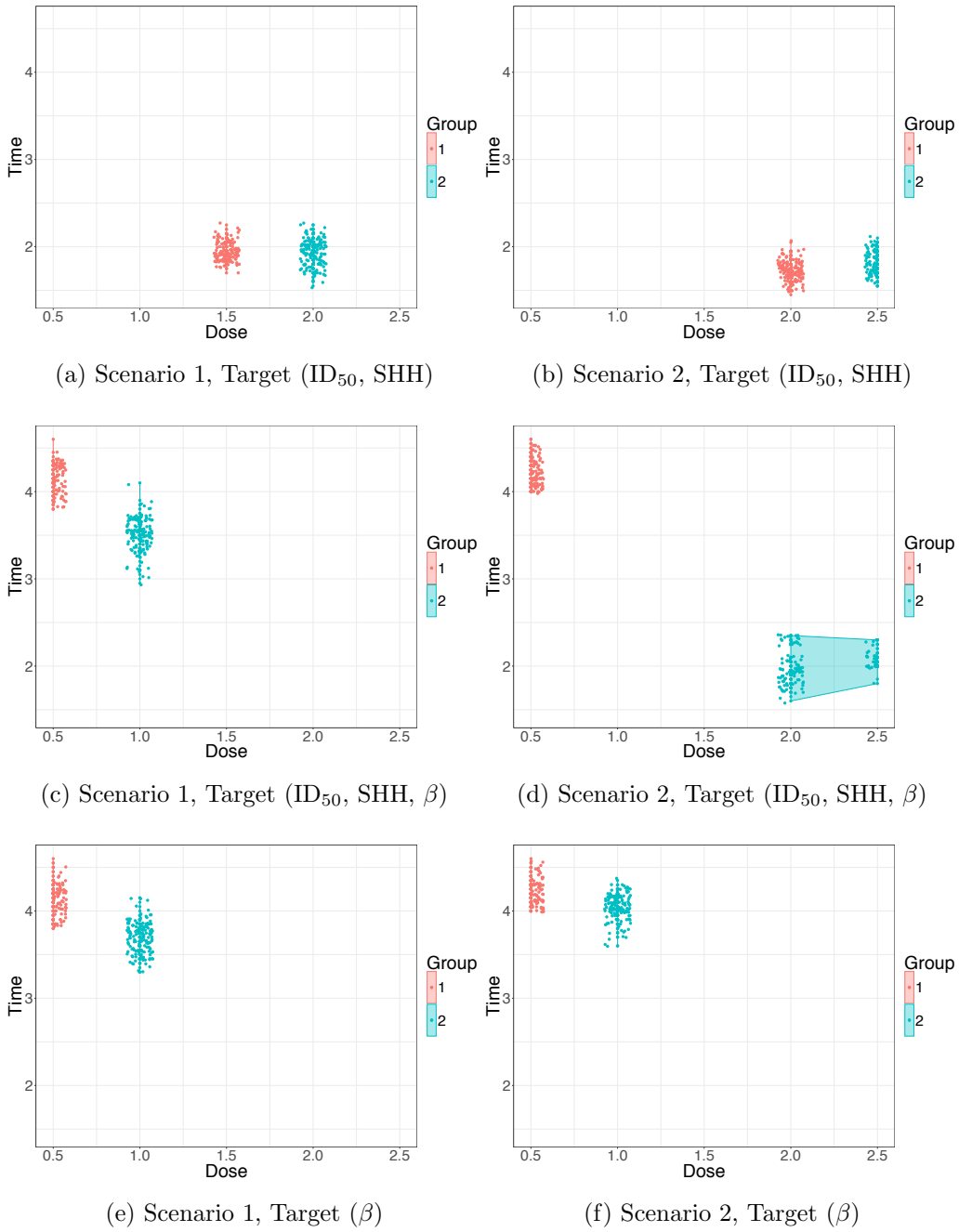


Figure 4: Convex hull plots demonstrating the dose-time pairing for each group, for the best 0.05% of designs according to the MAPE from the INSH algorithm, for Scenarios 1 and 2, when targeting each of (ID_{50}, SHH) , (ID_{50}, SHH, β) , and (β) .

315 *3.2. Performance of Optimal Designs*

316 *3.2.1. Scenario 1: Informative Prior Distributions*

317 Figures 5 and 6 show the performance of the two optimal designs (i.e., with respect
 318 to the EKLD and MAPE), for targeting the dose-response parameters, dose-response
 319 and transmission parameters, or the transmission parameter only (i.e., (ID_{50}, SHH) ,
 320 (ID_{50}, SHH, β) , or (β)), with informative prior distributions. Performance is assessed
 321 with respect to the bias in the median of the posterior distribution (i.e., posterior
 322 median - known parameter value used to simulate the experiment), and the posterior
 323 variance, of 200 simulated experiments.

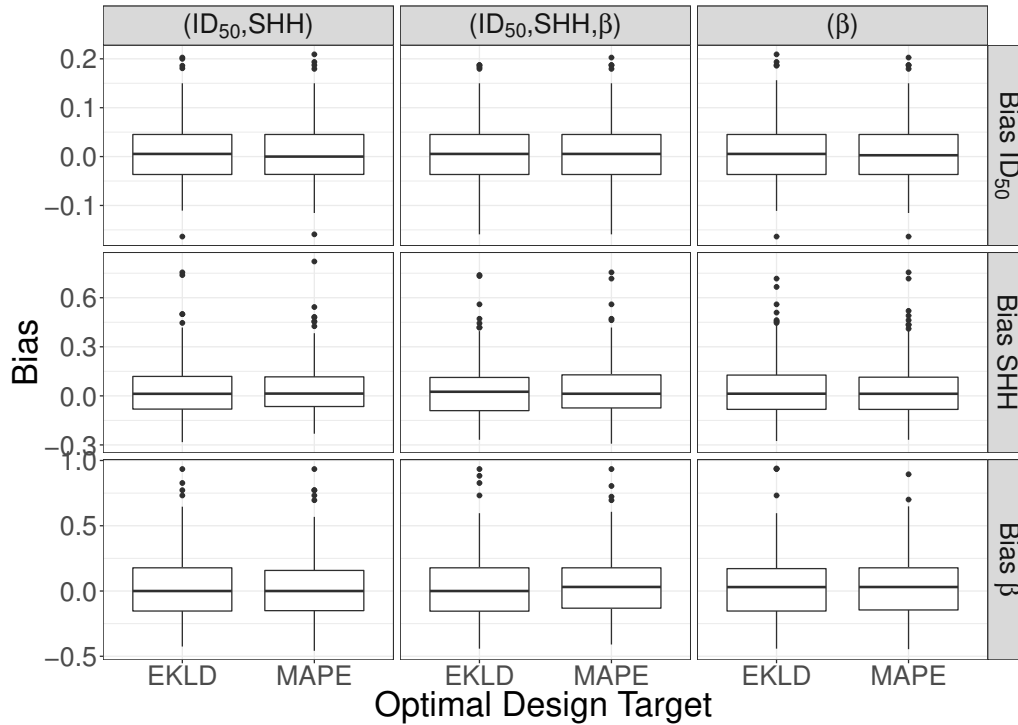


Figure 5: Scenario 1 (informative prior distributions). Boxplots of the posterior distribution median bias in estimates of each of ID_{50} , SHH and β (rows), corresponding to 200 simulated experiments, calculated at each of the optimal designs evaluated with respect to the EKLD and MAPE, when targeting each of the dose-response parameters, (ID_{50}, SHH) , transmission rate and dose-response parameters, (ID_{50}, SHH, β) , or only the transmission rate parameter (β) (columns).

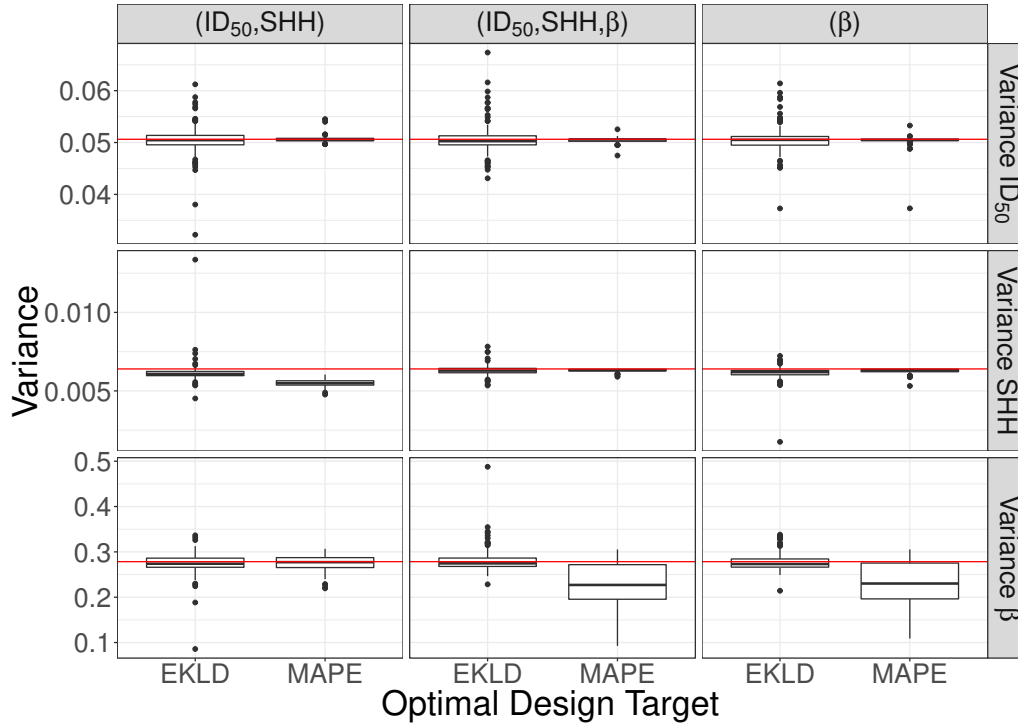


Figure 6: Scenario 1 (informative prior distributions). Boxplots of the variance of the posterior distribution of each of ID_{50} , SHH and β (rows), corresponding to 200 simulated experiments, calculated at each of the optimal designs evaluated with respect to the EKLD and MAPE, when targeting each of the dose-response parameters, (ID_{50}, SHH) , transmission rate and dose-response parameters, (ID_{50}, SHH, β) , or only the transmission rate parameter (β) (columns). The horizontal line in each figure corresponds to the prior variance.

3.2.2. Scenario 2: Uninformative Prior Distributions

Figures 7 and 8 show the performance of the two optimal designs (i.e., with respect to the EKLD and MAPE), for targeting the dose-response parameters, dose-response and transmission parameters, or the transmission parameter only (i.e., (ID_{50}, SHH) , (ID_{50}, SHH, β) , or (β)), with uninformative prior distributions. Performance is assessed with respect to the bias in the median of the posterior distribution (i.e., posterior median - known parameter value used to simulate the experiment), and the posterior variance, of 200 simulated experiments.

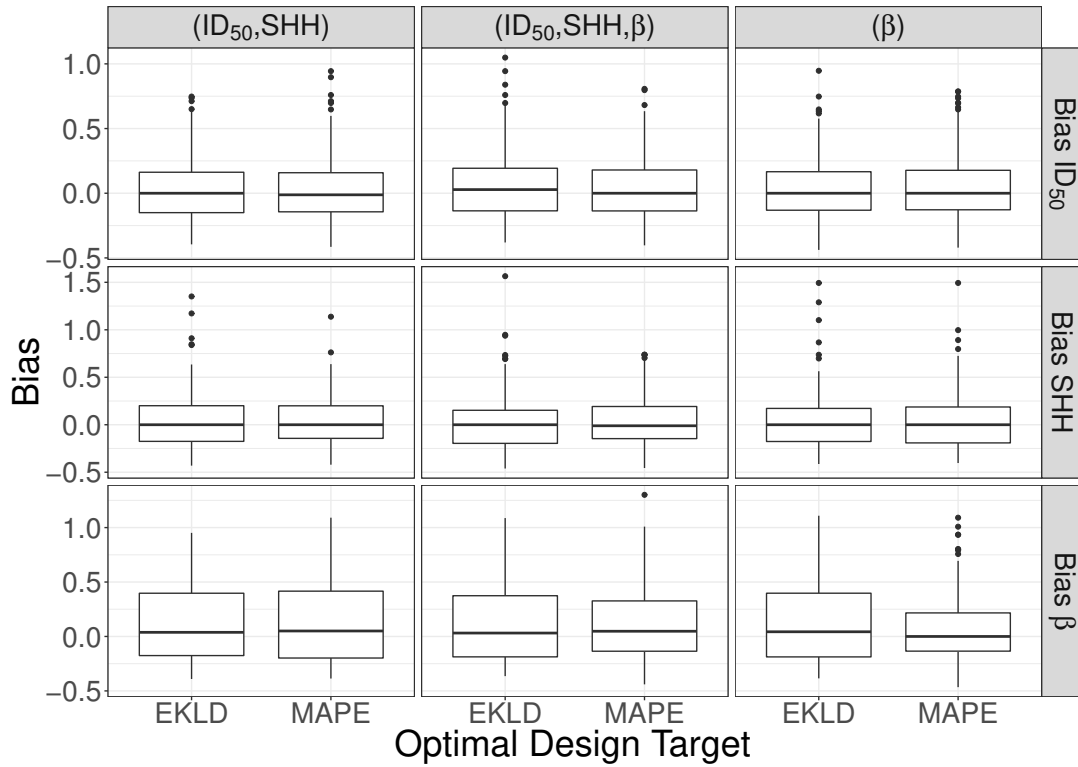


Figure 7: Scenario 2 (uninformative prior distributions). Boxplots of the posterior distribution median bias in estimates of each of ID_{50} , SHH and β (rows), corresponding to 200 simulated experiments, calculated at each of the optimal designs evaluated with respect to the EKLD and MAPE, when targeting each of the dose-response parameters, (ID_{50}, SHH) , transmission rate and dose-response parameters, (ID_{50}, SHH, β) , or only the transmission rate parameter (β) (columns).

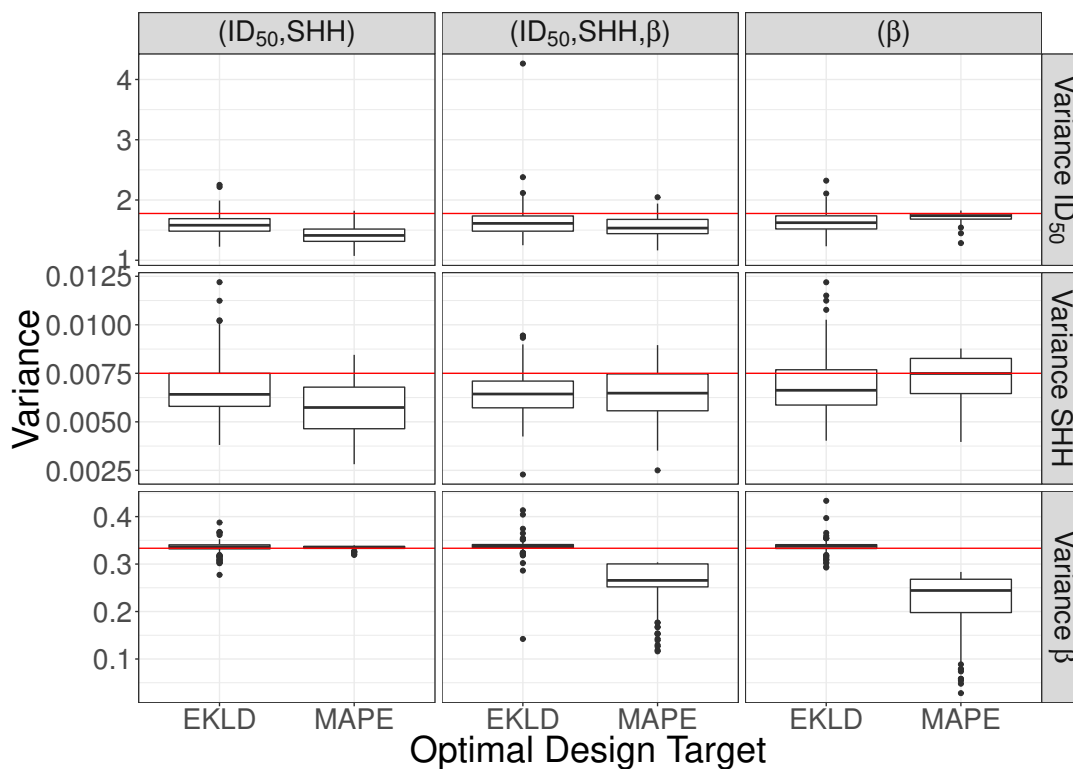


Figure 8: Scenario 2 (uninformative prior distributions). Boxplots of the variance of the posterior distribution of each of ID_{50} , SHH and β (rows), corresponding to 200 simulated experiments, calculated at each of the optimal designs evaluated with respect to the EKLD and MAPE, when targeting each of the dose-response parameters, (ID_{50}, SHH) , transmission rate and dose-response parameters, (α, δ, β) , or only the transmission rate parameter (β) (columns). The horizontal line in each figure corresponds to the prior variance.

332 4. Discussion

333 First of all, we wish to reiterate that the results here are prior-specific, and
 334 therefore different trends may be apparent when considering other prior distributions
 335 than those we have considered here.

336 The designs returned under the two different utility functions in Figures 3 and 4
 337 show distinct differences. In particular, the EKLD designs consistently prefer more
 338 groups (with less replicates in each), whereas the MAPE designs prefer more repli-

339 cates within less groups. The designs under the EKLD each show a similar pattern,
340 with low-dose groups being observed at a marginally later observation time (around
341 1.5-2 days post-inoculation), while groups that receive a larger dose are observed
342 earlier (around 0.85-1.25 days post-inoculation). The marginally later observation
343 time in the low-dose groups is indicative of the smaller probability of colonisation
344 in these groups, thus, suggesting it is beneficial to wait marginally longer than the
345 mean time to progress through the exposed classes (≈ 1 day), in order to successfully
346 observe the colonised chickens. The groups receiving larger doses can feasibly be ob-
347 served earlier, as there are a greater number of chickens that will be colonised (and
348 so we will have a negligible probability of observing no colonised chickens), while also
349 avoiding the possibility of transmission occurring.

350 In contrast, the MAPE designs are all preferentially allocating chickens to only
351 two groups, and show obvious differences depending on which parameter combina-
352 tions are of interest. Designs considering only the dose-response relationship (i.e.,
353 ID_{50} and SHH) are allocated to relatively small doses, and observed at later obser-
354 vation times (note that with the Erlang(2,2) distribution of time to pass through
355 the exposed classes, there is approximately a 90% chance of having progressed to
356 the infectious class by 2 days post-inoculation). When considering only the trans-
357 mission rate parameter, β , the designs are vastly different – with lower doses and
358 later observation times, allowing the potential for more transmission events to occur
359 and sufficient time to observe a second-wave of infectious chickens that would likely
360 be due to transmission. Finally, when considering both the dose-response relation-
361 ship and transmission dynamics, the designs attempt to balance the two previous
362 extremes. Under this example of informative prior distributions, the design resem-
363 bles that of considering only the transmission rate parameter, suggesting that more
364 information can be obtained about β than could be obtained for the ID_{50} or SHH.
365 This can be observed in the posterior variances in Figure 8, where the variance for
366 these dose-response parameters resembles both that of the EKLD designs, and the

367 prior variance, however there is a considerable improvement in the posterior vari-
368 ance for β compared to both the EKLD and prior variance. Note that there are no
369 distinct differences in the posterior bias estimates under the designs from the two
370 utility functions. Under the uninformative prior distribution however, we can see
371 that the optimal design is to actually allocate our resources between these two re-
372 gions – one group with a low-dose and late observation time in order to learn about
373 the transmission dynamics, and a second group with an earlier observation time and
374 a higher-dose in order to learn about the dose-response parameters.

375 Figures 6 and 8 demonstrate the posterior variance for each parameter, having
376 conducted the experiment under each of the different optimal designs, compared
377 to the variances of the prior distribution. Again, it appears as though the MAPE
378 designs outperform the EKLD designs – that is, the posterior distributions have
379 smaller variance, on average. In fact, in some cases, the posterior variance under
380 the EKLD designs appears marginally worse than that of the prior distribution –
381 suggesting that this allocation of resources provides no further information about the
382 system than was achievable under the prior distribution. The only instances that
383 the EKLD designs out-perform the MAPE designs appear to be with regards to the
384 slope-at-half-height of the dose-response relationship. Under the uninformative prior
385 distributions, the posterior variance of SHH is worse under the MAPE design than the
386 corresponding EKLD design, once consideration is also given to the transmission rate
387 parameter β (a marginal difference for (ID_{50}, SHH, β) , however more notable when
388 considering only (β)). Furthermore, the EKLD design appears to outperform the
389 MAPE design with respect to the posterior variance of ID_{50} when considering *only* β
390 – however, this is not unexpected as the MAPE design is targeting only β . Note that
391 each case where EKLD outperforms the MAPE, is where MAPE is not targeting the
392 parameter which has a larger posterior variance. The larger variances in each case are
393 made up by considerably reduced variance for the parameter of interest, compared
394 to the EKLD design. This suggests that the MAPE utility is clearly prioritising the

395 parameter of direct interest, and sacrifices estimating other parameters well in order
396 to gain improved accuracy for those parameters under consideration. Conversely,
397 the posterior variances evaluated at the EKLD designs do not appear to change
398 considerably when targeting different parameter combinations – not surprising, since
399 the designs returned under various scenarios for the EKLD utility were all very
400 similar. Thus, if only a subset of the model parameters are of interest, it appears
401 as though these can be more accurately targeted using the MAPE utility, rather
402 than the EKLD utility. Similar patterns exist in the informative scenarios, but to a
403 lesser degree (as there is a smaller margin for improvement) – in particular, note the
404 improved posterior variances for β under the MAPE designs, in the scenarios where
405 β is targeted, compared to the EKLD designs.

406 5. Conclusion

407 Group dose-response challenge experiments are routinely used to assess safe, ef-
408 fective, or hazardous doses of a substance. However, the possibility for transmission
409 can lead to incorrect estimation of the dose-response relationship. Here, we have
410 utilised optimal experimental design theory to demonstrate how to pre-determine a
411 suitable experimental design in order to target different aspects of the dose-response
412 relationship, or transmission dynamics.

413 Within the experimental design framework, the Mean Absolute Percentage Er-
414 ror (MAPE) appears to be a suitable alternative to the Expected Kullback-Leibler
415 Divergence (EKLD) as a choice of utility, in some situations, when evaluating op-
416 timal designs for the purpose of parameter inference. The designs evaluated under
417 the EKLD and MAPE have quite distinct features, most notably in the number of
418 preferred groups, which appears to correlate with better estimation of targeted pa-
419 rameters under the MAPE designs. It appears as though by allocating all subjects
420 to only two groups, we obtain more certain estimates of the dose-response relation-
421 ship at those doses, by reducing the uncertainty within each group. However, this

422 often comes at the cost of reduced information about other parameters that were not
423 directly being targeted – thus careful consideration needs to be given at the design
424 stage to the dynamics that are of interest when using the MAPE utility.

425 With regards to the MAPE designs, if there is interest in the transmission rate as
426 well as the dose-response relationship, then resources are directly allocated to esti-
427 mating the transmission rate. However, the amount of resources that should be used
428 to estimate the transmission rate parameter is governed by the level of prior informa-
429 tion that is available for the parameters. If we have informative prior distributions
430 for the dose-response parameters, then all resources are allocated to estimating the
431 transmission rate parameter (i.e., lower doses and late observation times). Inherently,
432 some information will still be available on the dose-response relationship from this
433 design, however the quantity of information that can be obtained about the trans-
434 mission rate parameter is greater than that regarding the dose-response relationship.
435 Conversely, if we have less-informative prior distributions on each parameter, then
436 the resources are allocated between the two regions – targeting the transmission
437 rate parameter (low dose and late observation time), or the dose-response param-
438 eters (higher dose and an earlier observation time), with a trade-off between the
439 information gain for each aspect of the underlying dynamic.

440 Here, we have used state-of-the-art experimental design methodology to provide
441 a tool to design group dose-response challenge experiments in the presence of trans-
442 mission. Code to implement this method in `MATLAB` is available as Supplementary
443 Material.

444 **Author Contributions**

445 DJP produced code and results, and drafted the manuscript. NGB, JVR and
446 JT conceived the study, and helped draft the manuscript. All authors gave final
447 approval for publication.

448 **Acknowledgements**

449 JVR acknowledges the support of the ARC (Future Fellowship FT130100254;
450 CoE ACEMS) and the NHMRC (CRE PRISM²). The authors would like to thank
451 Andrew Conlan and Andrew Grant (Department of Veterinary Medicine, University
452 of Cambridge), for their advice regarding the modelling, and the technical aspects
453 of dosing with infectious bacteria, respectively.

454 **6. Appendix**

455 *6.1. Algorithms*

Algorithm 1 ABC Algorithm: Fixed tolerance

Input: Observed data \mathbf{x} , simulated data $\mathbf{y} = (\mathbf{y}^1, \dots, \mathbf{y}^N)$, corresponding parameter values $\boldsymbol{\theta}^i, i = 1, \dots, N$, and tolerance ϵ .

- 1: Evaluate discrepancies $\rho^i = \rho(\mathbf{y}, \mathbf{x}^i)$, creating particles $\{\boldsymbol{\theta}^i, \rho^i\}$ for $i = 1, \dots, N$.
- 2: Using the posterior sample of parameters $\boldsymbol{\theta}^i$ such that $\rho^i < \epsilon$, evaluate utility.

Output: Utility for current design, having observed \mathbf{x} , $U(d, \mathbf{x})$.

Algorithm 2 ABCdE Algorithm

- 1: Choose grid over the parameter space for the discrete estimate of the utility, number of simulations N_{pre} , and tolerance ϵ .
- 2: Sample N_{pre} parameters $\boldsymbol{\theta}$ from $p(\boldsymbol{\theta})$.
- 3: For each of the N_{pre} parameters, and under every design d in the design space \mathcal{D} , simulate process and store $X_{N_{pre} \times |\mathcal{D}|}(\boldsymbol{\theta}, d)$.
- 4: **for** $i = 1$ to $|\mathcal{D}|$ **do**
- 5: Consider the unique rows of data $Y(\boldsymbol{\theta}, d^i) = \text{unique}(X(\boldsymbol{\theta}, d^i))$.
 Note: We let K^i be the number of such unique data, and n_{k^i} be the number of repetitions of the $k^{i^{th}}$ unique data, for $k^i = 1, \dots, K^i$.
- 6: **for** $k^i = 1$ to K^i **do**
- 7: Pass ‘observed data’ $\mathbf{y}^{k^i} = [Y(\boldsymbol{\theta}, d^i)]_{k^i}$, ‘simulated data’ $X(\boldsymbol{\theta}, d^i)$, N_{pre} sampled parameters, and tolerance ϵ to Algorithm 1, and return contribution $U(\mathbf{y}^{k^i}, d^i)$ to the expected utility, for $k^{i^{th}}$ unique datum (‘observed data’) and i^{th} design.
- 8: **end for**
- 9: Store $u(d^i) = \frac{1}{N} \sum_{k^i} n_{k^i} U(\mathbf{y}^{k^i}, d^i)$; the average utility over all parameters and data for design d^i .
- 10: **end for**

Output: The optimal design $d^* = \underset{d \in \mathcal{D}}{\operatorname{argmax}}(u(d))$.

Algorithm 3 INSH Algorithm

- 1: Choose an initial set of designs. D (e.g., a coarse grid of design points across the design space, or randomly sample).
- 2: Specify the number of generations (iterations) of the algorithm W , a perturbation function $f(d | d')$, and the acceptance criteria.
- 3: **for** $w = 1$ to W **do**
- 4: For each design $d^i \in D$, sample parameters $\boldsymbol{\theta} \sim p(\boldsymbol{\theta})$, and simulate data \boldsymbol{x}^i from the model.
- 5: Evaluate utility $u(d^i)$, for each design $d^i \in D$.
- 6: Set D' to be the designs which satisfy the acceptance criteria, and the current optimal design d^* (even if it occurred in a previous generation).
- 7: Sample m designs from $f(d | d')$, for each $d' \in D'$. Set D to be these newly sampled designs.
- 8: **end for**

Output: Set of designs d , and corresponding utilities $u(d)$ (and hence, the optimal design $d^* = \underset{d \in \mathcal{D}}{\operatorname{argmax}}(u(d))$).

456 *6.2. Derivation of P_{inf} Approximation.*

Consider the confluent hypergeometric function,

$${}_1F_1(\alpha, \alpha + \delta, -D) = \int_0^1 e^{-Dt} \frac{\Gamma(\alpha + \delta)}{\Gamma(\alpha)\Gamma(\delta)} t^{\alpha-1} (1-t)^{\delta-1} dt.$$

Let $t = y/\delta$, and hence $dt = dy/\delta$. Then we have,

$${}_1F_1(\alpha, \alpha + \delta, -D) = \int_0^\delta e^{-yD/\delta} \frac{\Gamma(\alpha + \delta)}{\Gamma(\alpha)\Gamma(\delta)} \left(\frac{y}{\delta}\right)^{\alpha-1} \left(1 - \left(\frac{y}{\delta}\right)\right)^{\delta-1} \frac{dy}{\delta}.$$

For large δ , $(1 - (y/\delta))^{\delta-1}$ is approximately equal to e^{-y} . Hence we have,

$${}_1F_1(\alpha, \alpha + \delta, -D) \approx \int_0^\delta e^{-yD/\delta} \left[\frac{\Gamma(\alpha + \delta)}{\delta^\alpha \Gamma(\delta)} \right] \left(\frac{y^{\alpha-1}}{\Gamma(\alpha)} \right) e^{-y} dy.$$

Employing Stirling's approximation to the expression inside the square brackets, we get,

$$\begin{aligned}
\frac{\Gamma(\alpha + \delta)}{\delta^\alpha \Gamma(\delta)} &\approx \frac{\sqrt{2\pi}(\alpha + \delta)^{\alpha+\delta-1/2} e^{-\alpha-\delta}}{\sqrt{2\pi}(\delta)^{\delta-1/2} e^{-\delta}} \times \frac{1}{\delta^\alpha} \\
&= \frac{(\alpha + \delta)^{\alpha+\delta-1/2} e^{-\alpha}}{(\delta)^{\alpha+\delta-1/2}} \\
&= e^{-\alpha} \left(1 + \frac{\alpha}{\delta}\right)^{\alpha+\delta-1/2} \\
&= 1,
\end{aligned}$$

457 since $(1 + \frac{\alpha}{\delta})^{\alpha+\delta-1/2}$ is approximately equal to e^α for large δ , and small α relative to
458 δ .

459 Note, Stirling's Approximation for the gamma function is: $\Gamma(z) = \sqrt{(2\pi/z)}(z/e)^z(1+$
460 $\mathcal{O}(1/z))$. The error of order $1/z$ is ignored since we consider large β .

Hence, we have,

$$\begin{aligned}
{}_1F_1(\alpha, \alpha + \delta, -D) &\approx \int_0^\delta e^{-yD/\delta} \left(\frac{y^{\alpha-1}}{\Gamma(\alpha)}\right) e^{-y} dy \\
&= \int_0^\delta e^{-y(1+D/\delta)} \left(\frac{y^{\alpha-1}}{\Gamma(\alpha)}\right) dy.
\end{aligned}$$

Let $u = y(1 + \frac{D}{\delta})$, and hence $dy = (1 + \frac{D}{\delta})^{-1} du$. Then, we have,

$$\begin{aligned}
{}_1F_1(\alpha, \alpha + \delta, -D) &\approx \int_0^{\delta+D} \left(\frac{u}{(1 + \frac{D}{\delta})}\right)^{\alpha-1} \frac{e^{-u}}{\Gamma(\alpha)} \frac{du}{(1 + \frac{D}{\delta})} \\
&= \left(1 + \frac{D}{\delta}\right)^{-\alpha} \int_0^{\delta+D} \frac{e^{-u} u^{\alpha-1}}{\Gamma(\alpha)} du.
\end{aligned}$$

Since $\frac{e^{-u} u^{\alpha-1}}{\Gamma(\alpha)}$ is the pdf for a random variable with a Gamma($\alpha, 1$) distribution, and for large δ ,

$$\int_0^{\delta+D} \frac{e^{-u} u^{\alpha-1}}{\Gamma(\alpha)} du \approx \int_0^\infty \frac{e^{-u} u^{\alpha-1}}{\Gamma(\alpha)} du = 1,$$

we get that,

$${}_1F_1(\alpha, \alpha + \delta, -D) \approx \left(1 + \frac{D}{\delta}\right)^{-\alpha}.$$

461 Hence, given dose D , and model parameters α and δ , we can write the probability
462 of infection as,

$$P_{\text{inf}}(D; \alpha, \delta) \approx 1 - \left(1 + \frac{D}{\delta}\right)^{-\alpha}. \quad (7)$$

463 *6.3. Results: INSH Algorithm*

464 Figures 9 and 10 shows the progression of the INSH algorithm towards regions
465 of the design space of high-utility, for each of the four scenarios for both the EKLD
466 and (negative) MAPE.

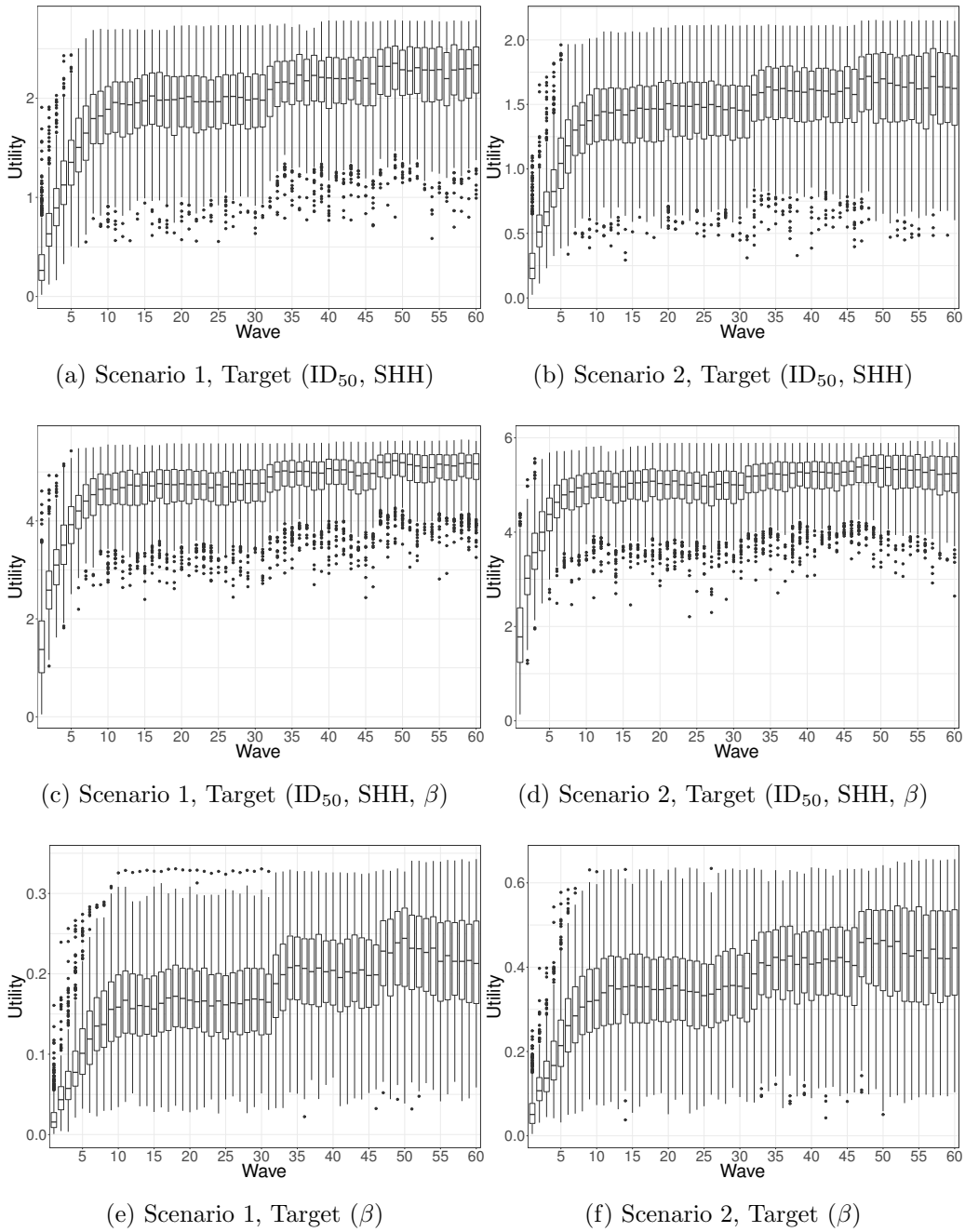


Figure 9: Estimated utility (EKLD) of designs considered at each wave of the INSH algorithm, for Scenarios 1 and 2, when targeting each of (ID_{50}, SHH) , (ID_{50}, SHH, β) , and β , respectively.

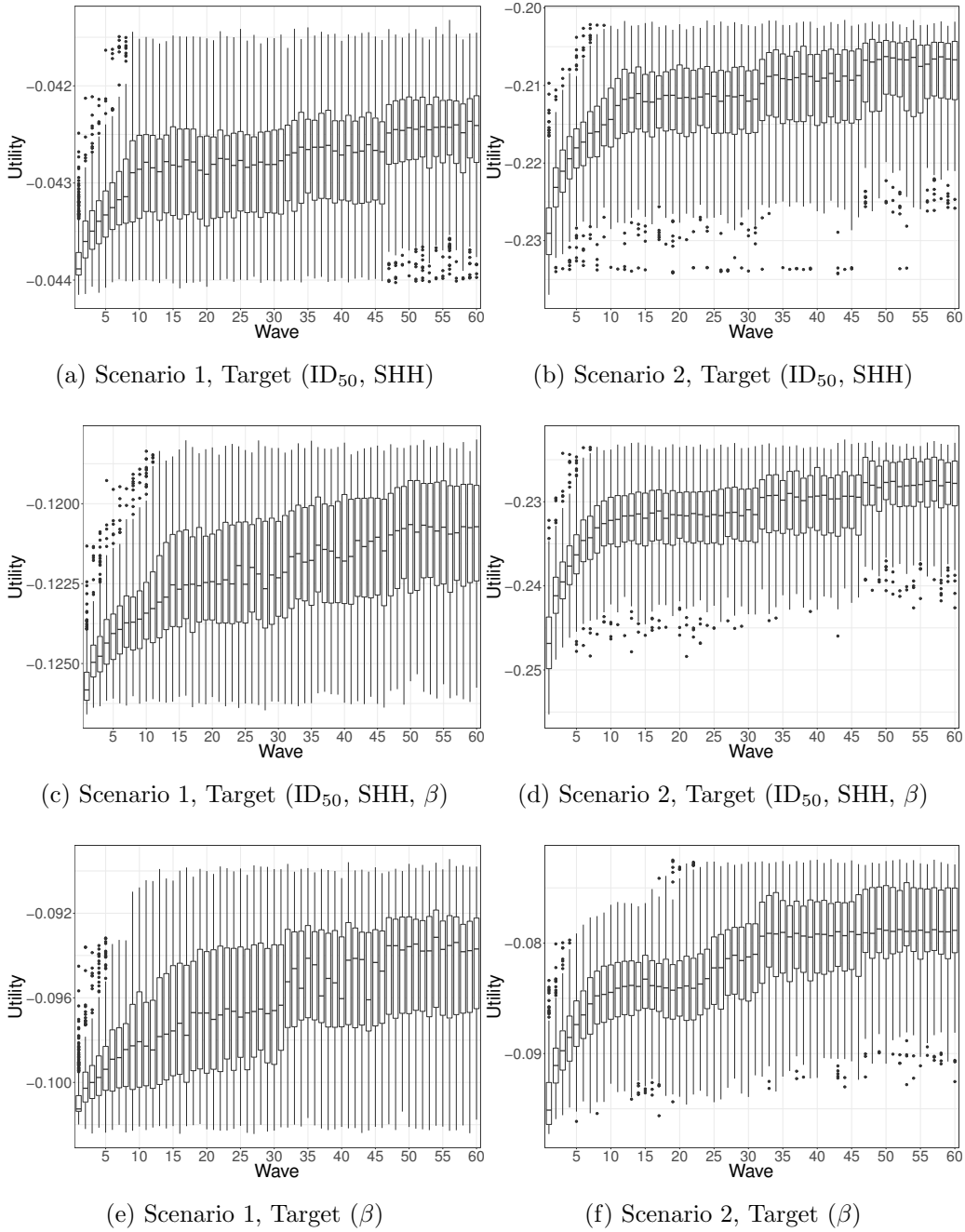


Figure 10: Estimated utility (MAPE) of designs considered at each wave of the INSH algorithm, for Scenarios 1 and 2, when targeting each of (ID_{50}, SHH) , (ID_{50}, SHH, β) , and β , respectively.

468 made up of each of $G = 2, 3, 4, 5$ groups, across each wave of the INSH algorithm.

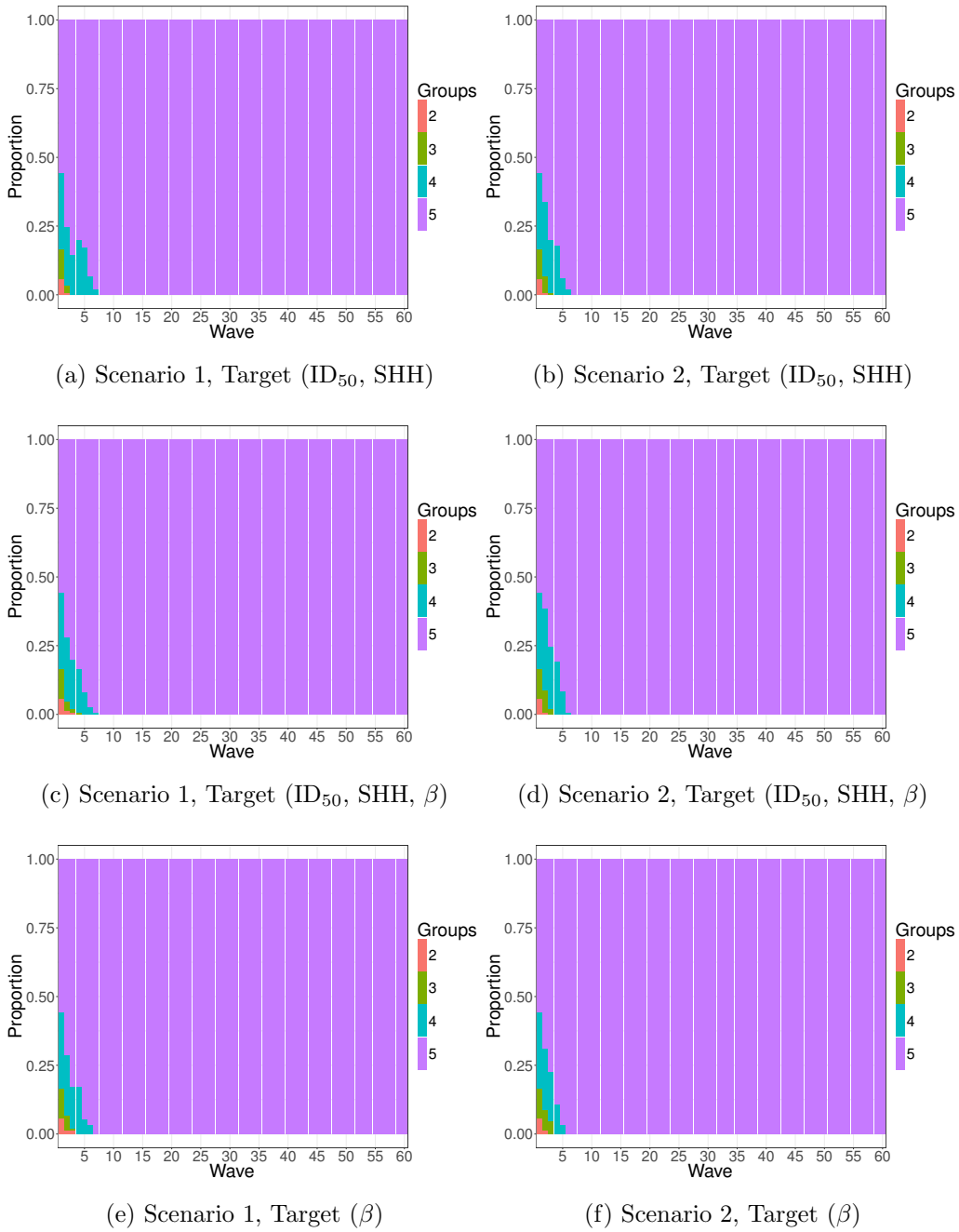


Figure 11: Proportion of the designs being considered at each wave of the INSH algorithm (EKLD), coloured by how many groups in each design, for Scenarios 1 and 2, when targeting each of (ID_{50}, SHH) , (ID_{50}, SHH, β) , and β , respectively.

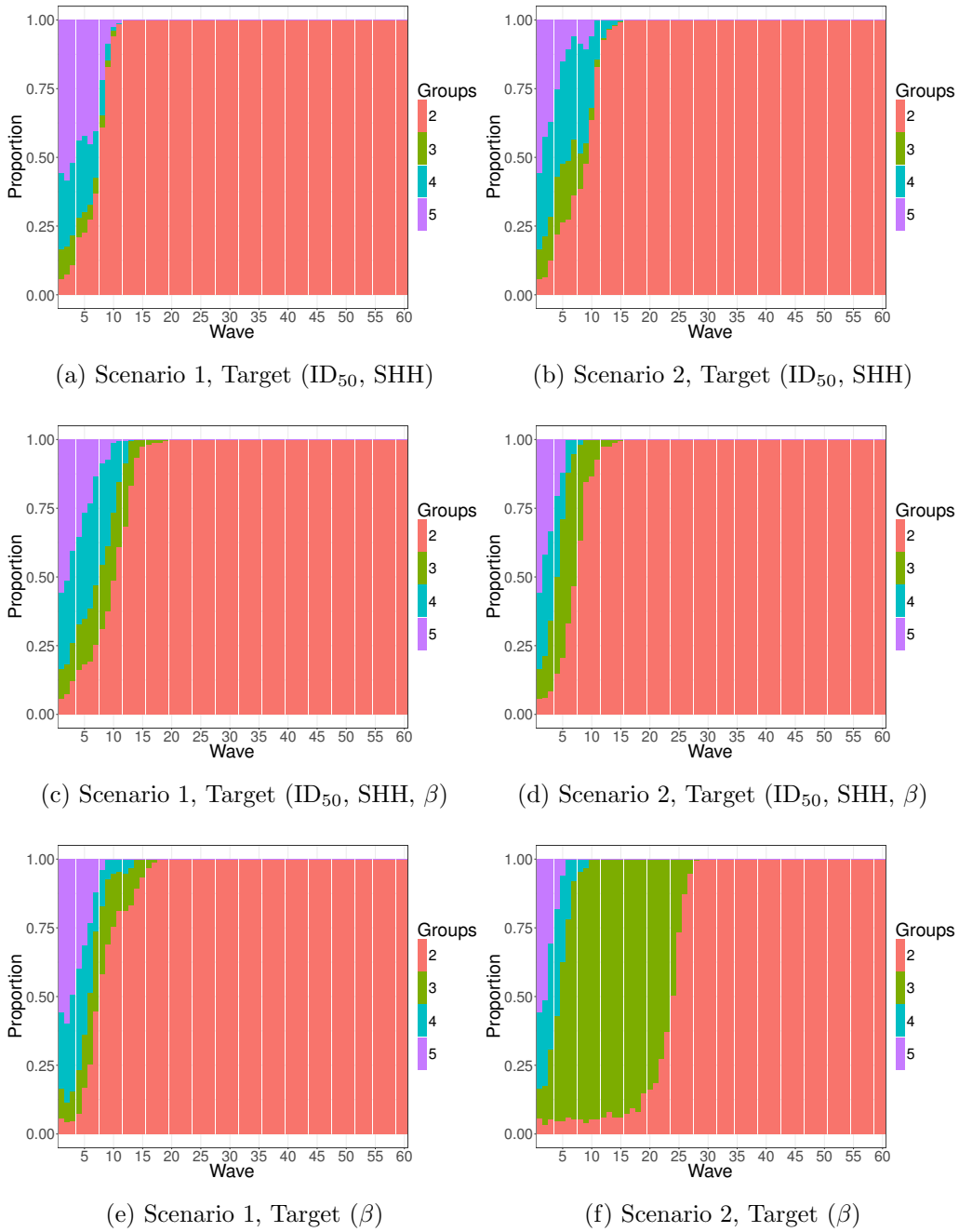


Figure 12: Proportion of the designs being considered at each wave of the INSH algorithm (MAPE), coloured by how many groups in each design, for Scenarios 1 and 2, when targeting each of (ID_{50}, SHH) , (ID_{50}, SHH, β) , and β , respectively.

469 **References**

- 470 [1] D. A. Berry. Bayesian clinical trials. *Nature Reviews Drug Discovery*, 5(1):
471 27–36, 2006.
- 472 [2] A. F. Brouwer, M. H. Weir, M. C. Eisenberg, R. Meza, and
473 J. N. S. Eisenberg. Dose-response relationships for environmentally me-
474 diated infectious disease transmission models. *PLoS Computational Bi-*
475 *ology*, 13(4):1–28, 04 2017. doi: 10.1371/journal.pcbi.1005481. URL
476 <https://doi.org/10.1371/journal.pcbi.1005481>.
- 477 [3] E. J. Calabrese and L. A. Baldwin. Toxicology rethinks its central belief. *Nature*,
478 421:691–692, 2003.
- 479 [4] K. Chaloner and I. Verdinelli. Bayesian experimental design: A review. *Statis-*
480 *tical Science*, 10(3):273–304, 1995.
- 481 [5] A. J. K. Conlan. personal communication, November 2017.
- 482 [6] A. J. K. Conlan, C. Coward, A. J. Grant, D. J. Maskell, and J. R. Gog. *Campy-*
483 *lobacter jejuni* colonization and transmission in broiler chickens: a modelling
484 perspective. *Journal of The Royal Society Interface*, 4(16), 2007.
- 485 [7] A. J. K. Conlan, J. E. Line, K. Hiett, C. Coward, P. M. Van Diemen, M. P.
486 Stevens, M. A. Jones, J. R. Gog, and D. J. Maskell. Transmission and dose-
487 response experiments for social animals: a reappraisal of the colonization biology
488 of *Campylobacter jejuni* in chickens. *Journal of The Royal Society Interface*, 8:
489 1720–1735, 2011.
- 490 [8] A. R. Cook, G. J. Gibson, and C. A. Gilligan. Optimal observation times in
491 experimental epidemic processes. *Biometrics*, 64(3):860–868, 2008.

- 492 [9] M. B. Dehideniya, C. C. Drovandi, and J. M. McGree. Optimal Bayesian design
493 for discriminating between models with intractable likelihoods in epidemiology.
494 *Computational Statistics & Data Analysis*, 124:277 – 297, 2018.
- 495 [10] C.C. Drovandi and A.N. Pettitt. Bayesian experimental design for models with
496 intractable likelihoods. *Biometrics*, 69:937–948, 2013.
- 497 [11] S. B. Duffull, G. Graham, K. Mengersen, and J. Eccleston. Evaluation of the
498 pre-posterior distribution of optimized sampling times for the design of phar-
499 macokinetic studies. *Journal of Biopharmaceutical Statistics*, 22:16–29, 2012.
- 500 [12] Food & Agriculture Organization of the United Nations and World Health Or-
501 ganization. Risk assessment of *Campylobacter spp.* in broiler chickens. Technical
502 report, Microbiological risk assessment series 12, 2009.
- 503 [13] A. J. Grant. personal communication, email, April 2018.
- 504 [14] *Code of Practice for the Housing and Care of Animals Bred, Supplied or Used*
505 *for Scientific Purposes*. Home Office UK, 2014.
- 506 [15] X. Huan and Y. M. Marzouk. Simulation-based optimal Bayesian experimental
507 design for nonlinear systems. *Journal of Computational Physics*, 232:288–317,
508 2013.
- 509 [16] P. Marjoram, J. Molitor, V. Plagnol, and S. Tavaré. Markov chain Monte Carlo
510 without likelihoods. *PNAS*, 100(26):15324–15328, 2003.
- 511 [17] J. M. McGree, C. C. Drovandi, and A. N. Pettitt. A sequential Monte Carlo
512 approach to derive sampling times and windows for population pharmacokinetic
513 studies. *Journal of Pharmacokinetics and Pharmacodynamics*, 39:519–526, 2012.
- 514 [18] T. McKinley, A. R. Cook, and R. Deardon. Inference in epidemic models without
515 likelihoods. *The International Journal of Biostatistics*, 2009.

- 516 [19] A. M. Overstall and D. C. Woods. Bayesian design of experiments using Ap-
517 proximate Coordinate Exchange. *Technometrics*, 0(0):1–13, 2017.
- 518 [20] D. J. Price, N. G. Bean, J. V. Ross, and J. Tuke. On the efficient determination
519 of optimal Bayesian experimental designs using ABC: A case study in optimal
520 observation of epidemics. *Journal of Statistical Planning and Inference*, 172:
521 1–15, 2016.
- 522 [21] D. J. Price, N. G. Bean, J. V. Ross, and J. Tuke. An induced natural selec-
523 tion heuristic for finding Bayesian optimal experimental designs. *Computational*
524 *Statistics & Data Analysis*, 126:112–124, 2018.
- 525 [22] D. D. Ringoir, D. Szylo, and V. Korolik. Comparison of 2-day-old and 14-day-
526 old chicken colonization models for *Campylobacter jejuni*. *FEMS Immunology*
527 *& Medical Microbiology*, 47:155–158, 2007.
- 528 [23] J. V. Ross, D. E. Pagendam, and P. K. Pollett. On parameter estimation
529 in population models II: Multi-dimensional processes and transient dynamics.
530 *Theoretical Population Biology*, 75:123–132, 2009.
- 531 [24] E. G. Ryan, C. C. Drovandi, M. H. Thompson, and A. N. Pettitt. Towards
532 Bayesian experimental design for nonlinear models that require a large number
533 of sampling times. *Computational Statistics & Data Analysis*, 70:45–60, 2014.
- 534 [25] E. G. Ryan, C.C. Drovandi, J. M. McGree, and A.N. Pettitt. A review of modern
535 computational algorithms for Bayesian optimal design. *International Statistics*
536 *Review*, 2015.
- 537 [26] R. A. Saenz, S. C. Essen, S. M. Brookes, M. Iqbal, J. L. N. Wood, B. T. Grenfell,
538 J. W. McCauley, I. H. Brown, and J. Gog. Quantifying transmission of highly
539 pathogenic and low pathogenicity H7N1 avian influenza in turkeys. *PLoS One*,
540 2012.

- 541 [27] R. J. Tallarida and L. S. Jacob. *The Dose-Response Relation in Pharmacology*.
542 Springer-Verlag New York Inc., 1979.
- 543 [28] D. J. A. Toth, A. V. Gundlapalli, W. A. Schell, K. Bulmahn, T. E. Walton, C. W.
544 Woods, C. Coghill, F. Gallegos, M. H. Samore, and F. R. Adler. Quantitative
545 models of the dose-response and time course of inhalational anthrax in humans.
546 *PLoS Pathogens*, 9(8):1–18, 2013.
- 547 [29] T. J. W. M. Van Gerwe, A. Bouma, W. F. Jacobs-Reitsma, J. van den Broek,
548 D. Klinkenberg, J. A. Stegeman, and J. A. P. Heesterbeek. Quantifying trans-
549 mission of *Campylobacter* spp. among broilers. *Applied and Environmental Mi-*
550 *crobiology*, 71(10):5765–5770, 2005.
- 551 [30] H.J. Wearing, P. Rohani, and M. J. Keeling. Appropriate models for the manage-
552 ment of infectious diseases. *PLoS Medicine*, 2(7):e174, 2005. doi: 10.1371/jour-
553 nal.pmed.0020174.
- 554 [31] D. J. Wilson, E. Gabriel, A. J. H. Leatherbarrow, J. Cheesbrough, S. Gee,
555 E. Bolton, A. Fox, P. Fearnhead, C. Anthony Hart, and P. J. Diggle. Trac-
556 ing the source of campylobacteriosis. *PLoS Genetics*, 4(9):1–9, 09 2008. doi:
557 10.1371/journal.pgen.1000203.

Supplementary Material for Designing group dose-response studies in the presence of transmission

David J. Price^{a,b}, Nigel G. Bean^{c,d}, Joshua V. Ross^{c,d}, Jonathan Tuke^{c,d}

^a*Centre for Epidemiology and Biostatistics, Melbourne School of Population and Global Health, The University of Melbourne, VIC 3010, Australia*

^b*Victorian Infectious Diseases Reference Laboratory Epidemiology Unit at The Peter Doherty Institute for Infection and Immunity, The University of Melbourne and Royal Melbourne Hospital, VIC 3000, Australia*

^c*School of Mathematical Sciences, University of Adelaide, SA 5005, Australia*

^d*ARC Centre of Excellence for Mathematical & Statistical Frontiers, School of Mathematical Sciences, University of Adelaide, SA 5005, Australia*

1. Supplementary Results: Finer grid on dose-allocation

These supplementary results mirror those presented in the manuscript, however, here we consider both prior distributions placed on the parameters α and β directly, and a finer grid across the dose-allocation, in order to demonstrate the results that we can obtain should we be able to feasibly derive doses to this precision.

1.1. Prior Distributions

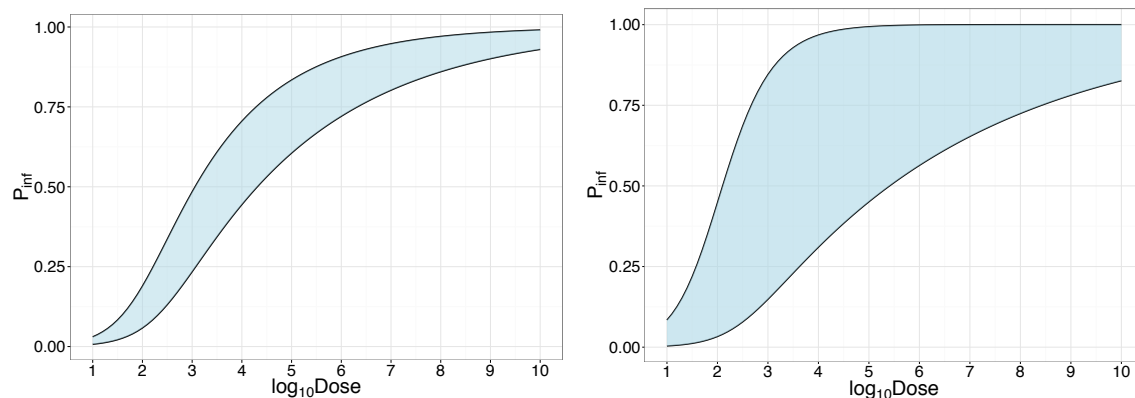
In the following examples, we consider two scenarios: 1) where we have a reasonably informative prior distribution, and 2) where we have a relatively uninformative prior distribution. Table S1 contains the choice of prior distribution for each parameter, in the two scenarios.

Table S1: Choice of prior distributions for dose-response model parameters, (α, δ) and transmission parameter β .

| Scenario | Parameter | | |
|----------|-----------------|------------------------|----------------------|
| | α | δ | β |
| 1 | $U(0.15, 0.25)$ | $\log -N(4.825, 0.25)$ | $\log -N(0.7, 0.25)$ |
| 2 | $U(0.10, 0.70)$ | $U(75, 250)$ | $U(1, 3)$ |

Email address: david.j.price@alumni.adelaide.edu.au (David J. Price)

Figures S1a and S1b demonstrate the resulting dose-response curves under the specified prior distributions for (α, δ) . The viable curves are demonstrated using the end points of the prior distribution for uniformly distributed parameters, and the (0.025, 0.975)-quantiles of the prior distribution otherwise.



(a) Dose-response relationship under informative prior distributions. (b) Dose-response relationship under uninformative prior distributions.

Figure S1: The shaded region demonstrates the prior-predictive dose-response relationship under (a) informative, or (b) uninformative prior distributions.

1.2. Design Space

Consider a scenario where we are limited by resources – e.g., a fixed number of chickens, doses or maximum time over which we may conduct the experiment. Specifically, assume we are able to dose at most $N = 40$ chickens. We are interested in determining optimal Bayesian experimental designs with respect to the number of groups to allocate the fixed number of subjects to, the dose to allocate to each group, and the time to sample each group. The ranges of these design parameters are presented in Table S2. Note, we are dealing with a social animal, and as such, subjects must be co-housed. That is, we assume that the chickens are allocated amongst at most five groups.

Table S2: Typical values of design parameters considered when determining the optimal experimental designs.

| Design aspect | Typical Values |
|---------------------------|---|
| Number of groups (G) | $\{2,3,4,5\}$ |
| Dose allocation (A) | $\{0.05,0.10,0.15,\dots,8.00\}$ \log_{10} CFU |
| Observation times (T) | $\{0.05,0.10,0.15,\dots,6.00\}$ days |

We consider only the number of groups G , rather than the number of groups and the number of chickens in each group – specifically, we assume that the $N = 40$ chickens are to be divided evenly among two, three, four or five groups (that is, 20, 13, 10 or 8 chickens per group). Note that throughout we refer to the dose in units of \log_{10} colony forming units (CFU), i.e., we refer to a dose of 10^4 CFU, as a dose of 4. We allow any number of groups to receive the same dose, and each group can have a different observation time – note that each individual within a group has the same dose and observation time.

2. Results

In the following, we consider two scenarios: 1) where we have an informative prior distribution on the model parameters, and 2) where we have an uninformative prior distribution. For both scenarios, we consider the optimal designs with respect to both 1) the EKLD, and 2) the MAPE. Furthermore, we also establish the optimal designs when we are interested in either 1) the dose-response parameters only, 2) the transmission rate parameter only, and 3) the dose-response and the transmission rate parameter. That is, in total, we consider 12 different sets of results. We present the optimal designs obtained via the INSH algorithm, in each example, and provide figures demonstrating the regions (with respect to the dose and observation time) that each group should be allocated to – akin to sampling windows considered in pharmacokinetic experiments (e.g., [1], [2], [3]). We describe these regions by taking the top n designs from the INSH algorithm output, and drawing a convex hull around each group (here, $n = 35$).

We demonstrate how well each design performs with regards to inference for all parameters. In particular, for 200 simulated experiments, we evaluate the bias (of the posterior median estimate) and variance of the posterior distributions evaluated under each design for each simulated experiment. The posterior distributions were evaluated using a standard ABC-rejection algorithm with 1,500,000 simulations, and a tolerance of $\epsilon = 0.25 \times G$.

Figures illustrating the convergence of the INSH algorithm – with respect to the number of designs of each group size being considered, and the utility of all designs under consideration at each wave – for each scenario are presented in Appendix 4.1.

2.1. Optimal Designs from the INSH Algorithm

The same setup for the INSH algorithm is used in these examples, as those reported in the main results.

Table S3 contains the resulting optimal experimental design for each scenario.

| Scenario | Utility | Target Parameters | G | Optimal Design: A: Dose (\log_{10} CFU); T: Obs. Time (days) |
|----------|---------|---------------------------|---|--|
| 1 | EKLD | (α, δ) | 5 | $A = (3.50, 3.95, 4.20, 4.25, 4.30)$ $T = (1.30, 1.40, 1.80, 1.55, 1.60)$ |
| 1 | MAPE | (α, δ) | 5 | $A = (3.60, 4.00, 4.20, 4.30, 4.65)$ $T = (1.35, 1.45, 1.90, 1.45, 1.55)$ |
| 1 | EKLD | (α, δ, β) | 5 | $A = (3.75, 3.90, 4.15, 4.20, 4.25)$ $T = (1.25, 1.35, 1.50, 1.70, 1.65)$ |
| 1 | MAPE | (α, δ, β) | 2 | $A = (2.50, 2.55)$ $T = (4.50, 4.25)$ |
| 1 | EKLD | (β) | 5 | $A = (4.00, 4.10, 4.25, 4.30, 4.35)$ $T = (1.35, 1.50, 1.80, 1.60, 1.40)$ |
| 1 | MAPE | (β) | 2 | $A = (2.40, 2.45)$ $T = (5.00, 4.90)$ |
| 2 | EKLD | (α, δ) | 5 | $A = (4.20, 4.45, 4.70, 5.05, 6.55)$ $T = (0.95, 0.95, 1.15, 1.10, 0.90)$ |
| 2 | MAPE | (α, δ) | 2 | $A = (3.25, 3.40)$ $T = (1.55, 1.75)$ |
| 2 | EKLD | (α, δ, β) | 5 | $A = (4.55, 4.65, 4.75, 5.00, 5.15)$ $T = (1.10, 1.05, 1.00, 0.95, 0.85)$ |
| 2 | MAPE | (α, δ, β) | 5 | $A = (2.20, 2.25, 3.25, 3.40, 3.50)$ $T = (3.05, 3.55, 1.70, 1.90, 1.70)$ |
| 2 | EKLD | (β) | 5 | $A = (4.45, 4.70, 4.85, 5.10, 6.25)$ $T = (1.05, 1.15, 1.10, 1.10, 0.85)$ |
| 2 | MAPE | (β) | 2 | $A = (1.95, 2.00)$ $T = (5.25, 5.00)$ |

Table S3: Optimal designs corresponding to two different scenarios ((1) informative and (2) uninformative prior distributions), according to two different utility functions (EKLD and MAPE), where the parameters of interest are either just the dose-response parameters (α, δ) , the transmission parameter (β) , or both the dose-response and transmission rate parameters (α, δ, β) .

Figures S2 and S3 show the dose and time combination for each group of the designs (i.e., the coloured groups 1 – G represent the G groups in the design). The figures show convex hulls around the “best” 35 designs with respect to the EKLD and MAPE (respectively). The designs have been jittered slightly so that one can identify where more design points for each group are clustered.

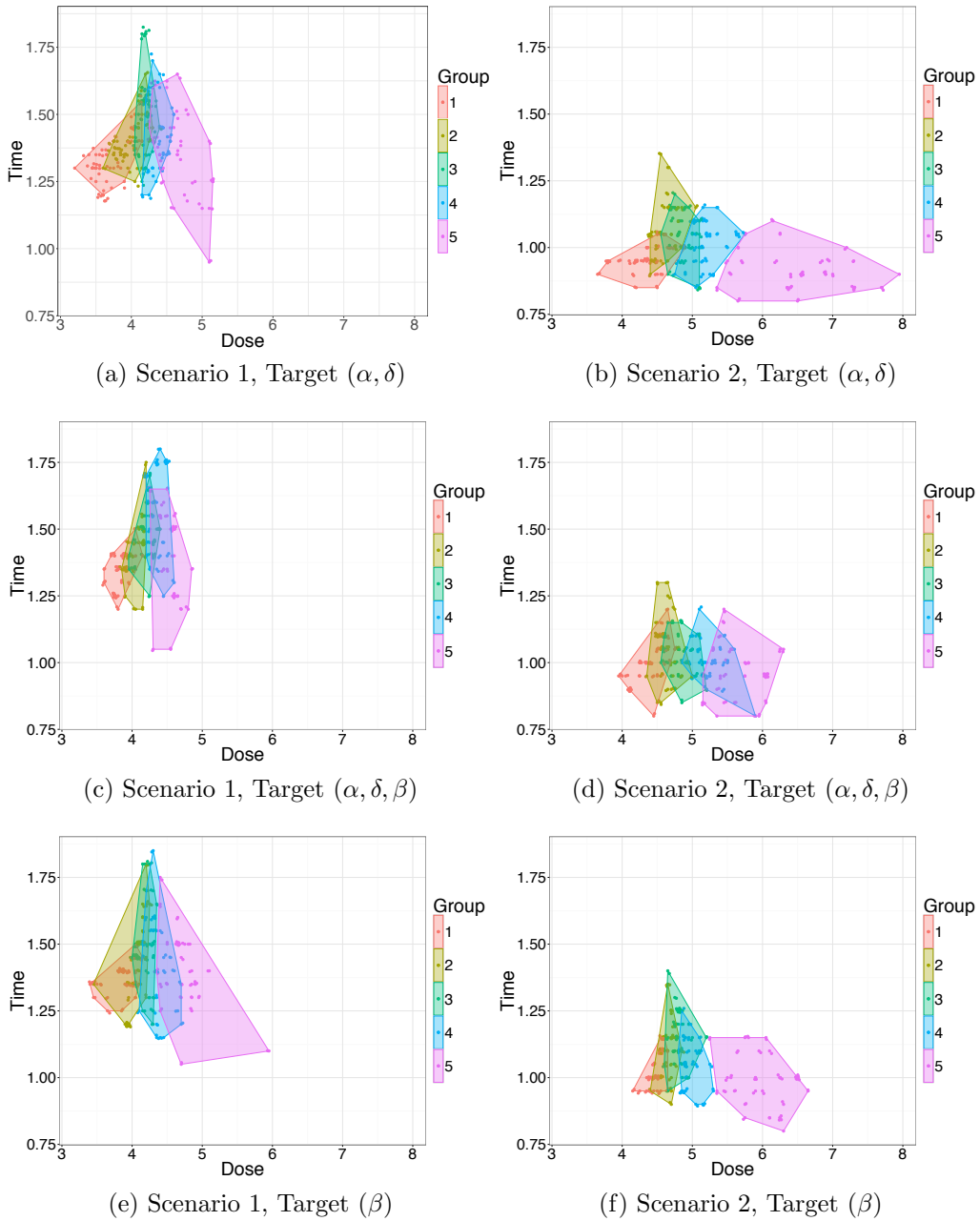


Figure S2: Convex hulls demonstrating the dose-time pairing for each group, for the 35 “best” designs according to the EKLD from the INSH algorithm, for Scenarios 1 and 2, when targeting each of (α, δ) , (α, δ, β) , and (β) .

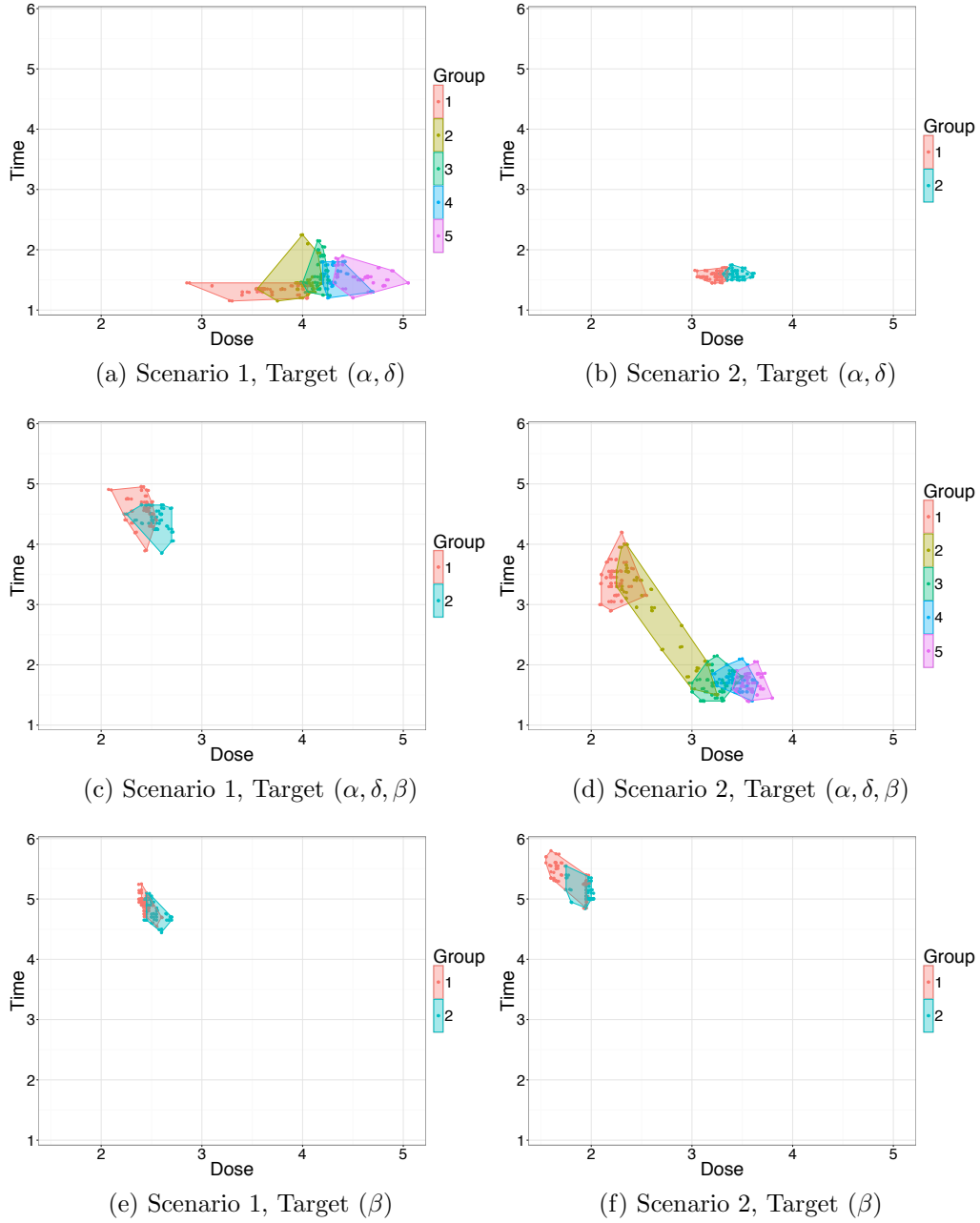


Figure S3: Convex hulls demonstrating the dose-time pairing for each group, for the 35 “best” designs according to the MAPE from the INSH algorithm, for Scenarios 1 and 2, when targeting each of (α, δ) , (α, δ, β) , and (β) .

2.2. Performance of Optimal Designs

2.2.1. Scenario 1: Informative Prior Distributions

Figures S4 and S5 show the performance of the two optimal designs (i.e., with respect to the EKLD and MAPE), for targeting the dose-response parameters, dose-response and transmission parameters, or the transmission parameter only (i.e., (α, δ) , (α, δ, β) , or (β)), with informative prior distributions. Performance is assessed with respect to the bias in the median of the posterior distribution (i.e., posterior median - known parameter value used to simulate the experiment), and the posterior variance, of 200 simulated experiments.

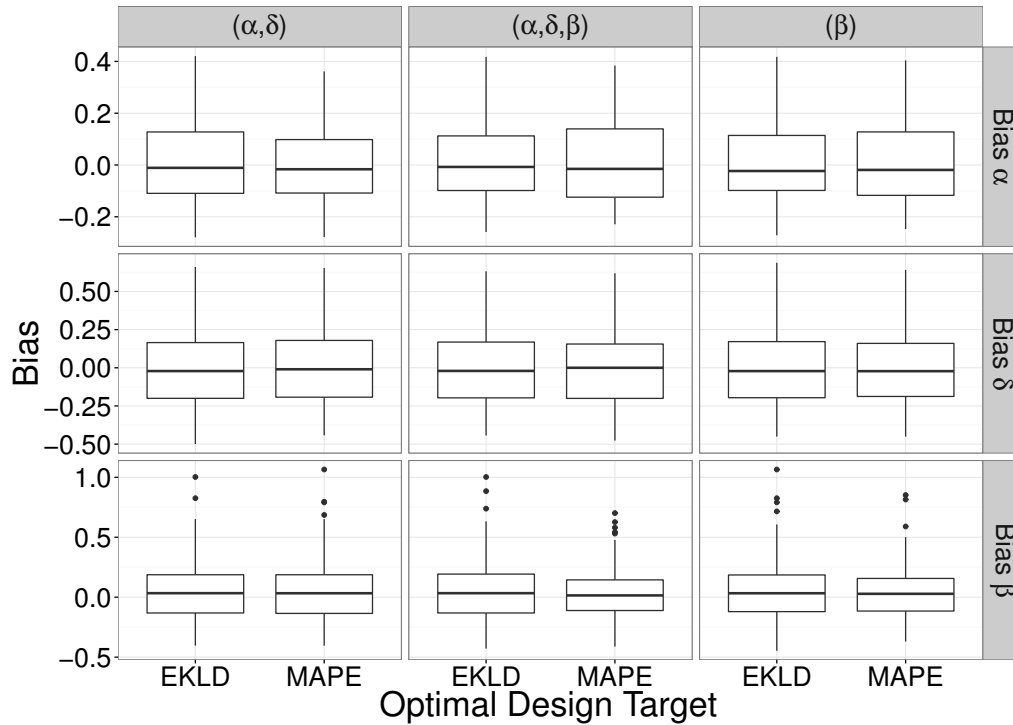


Figure S4: Scenario 1 (informative prior distributions). Boxplots of the posterior distribution median bias in estimates of each of α , δ and β (rows), corresponding to 200 simulated experiments, calculated at each of the optimal designs evaluated with respect to the EKLD and MAPE, when targeting each of the dose-response parameters, (α, δ) , transmission rate and dose-response parameters, (α, δ, β) , or only the transmission rate parameter (β) (columns).

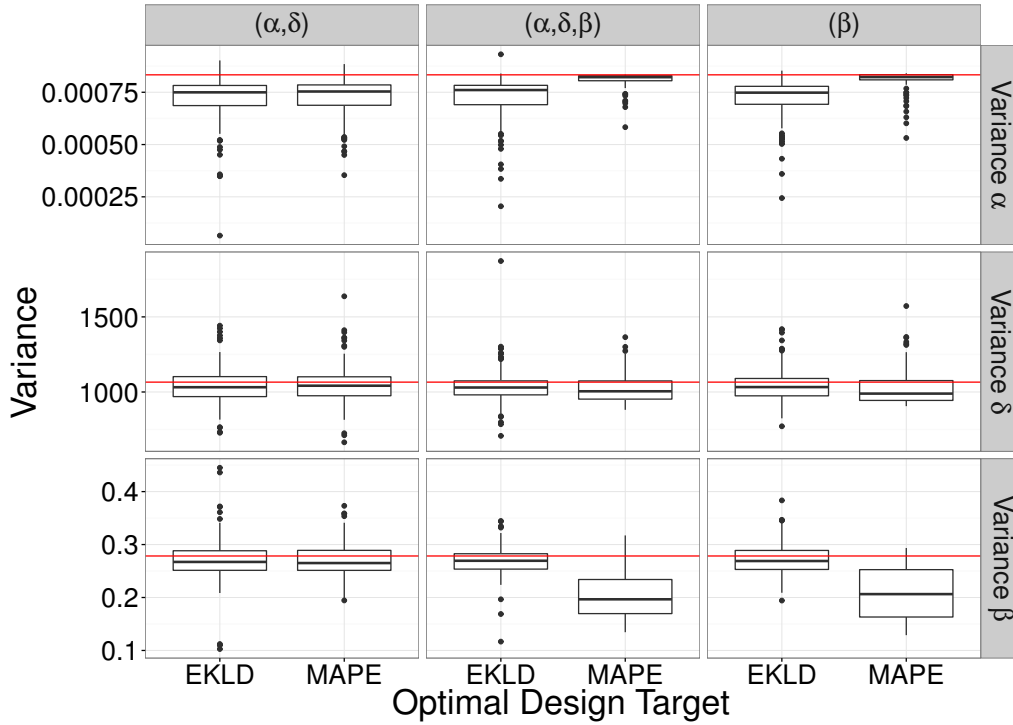


Figure S5: Scenario 1 (informative prior distributions). Boxplots of the variance of the posterior distribution of each of α , δ and β (rows), corresponding to 200 simulated experiments, calculated at each of the optimal designs evaluated with respect to the EKLD and MAPE, when targeting each of the dose-response parameters, (α, δ) , transmission rate and dose-response parameters, (α, δ, β) , or only the transmission rate parameter (β) (columns). The horizontal line in each figure corresponds to the prior variance.

2.2.2. Scenario 2: Uninformative Prior Distributions

Figures S6 and S7 show the performance of the two optimal designs (i.e., with respect to the EKLD and MAPE), for targeting the dose-response parameters, dose-response and transmission parameters, or the transmission parameter only (i.e., (α, δ) , (α, δ, β) , or (β)), with uninformative prior distributions. Performance is assessed with respect to the bias in the median of the posterior distribution (i.e., posterior median - known parameter value used to simulate the experiment), and the posterior variance, of 200 simulated experiments.

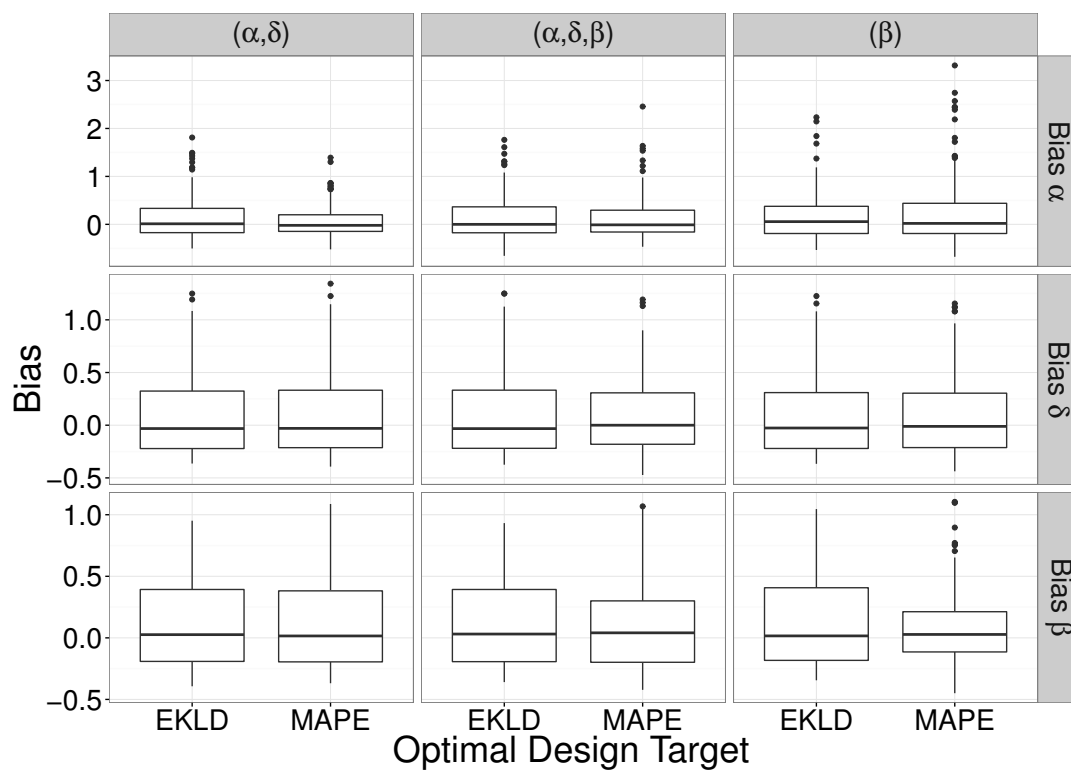


Figure S6: Scenario 2 (uninformative prior distributions). Boxplots of the posterior distribution median bias in estimates of each of α , δ and β (rows), corresponding to 200 simulated experiments, calculated at each of the optimal designs evaluated with respect to the EKLD and MAPE, when targeting each of the dose-response parameters, (α, δ) , transmission rate and dose-response parameters, (α, δ, β) , or only the transmission rate parameter (β) (columns).

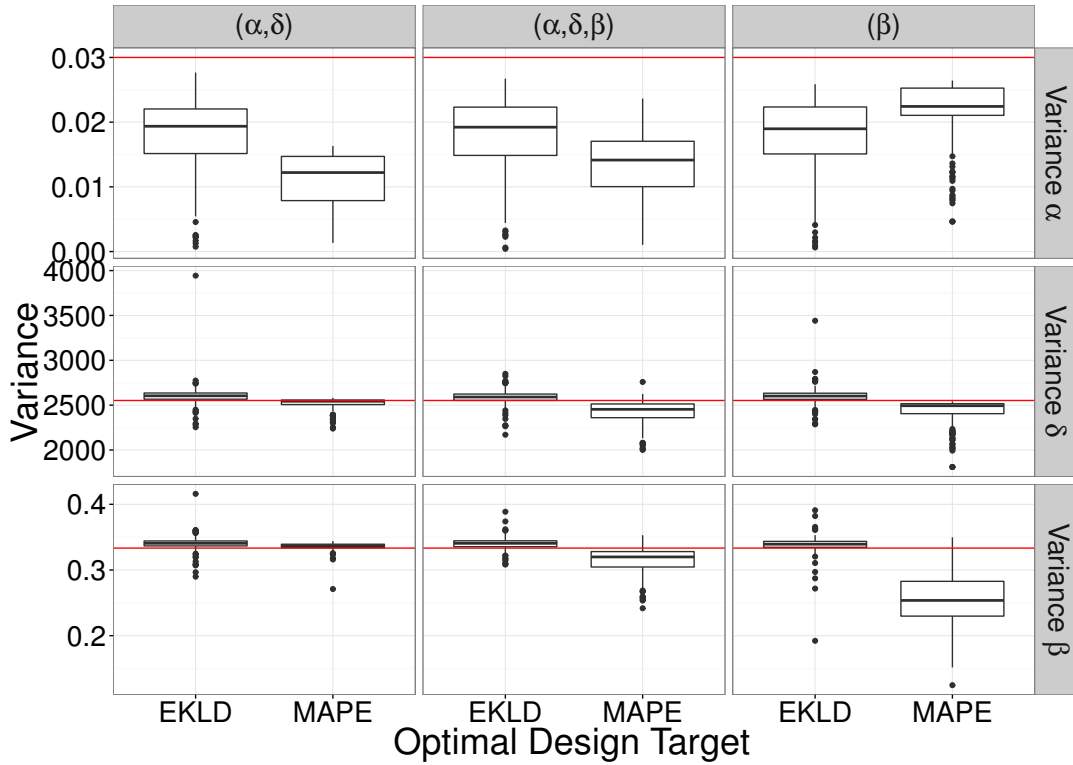


Figure S7: Scenario 2 (uninformative prior distributions). Boxplots of the variance of the posterior distribution of each of α , δ and β (rows), corresponding to 200 simulated experiments, calculated at each of the optimal designs evaluated with respect to the EKLD and MAPE, when targeting each of the dose-response parameters, (α, δ) , transmission rate and dose-response parameters, (α, δ, β) , or only the transmission rate parameter (β) (columns). The horizontal line in each figure corresponds to the prior variance.

3. Discussion

The designs that are obtained under the EKLD utility are demonstrated in Figure S2. In each case, the EKLD utility appears to suggest allocating the chickens amongst five groups, with doses that correspond to the prior ID_{50} . Note that the doses under the informative prior distribution are allocated across a narrower range compared to those for the uninformative prior distribution, corresponding to the increased prior belief in the location of the dose-response relationship. In Scenario 1 (informative prior distribution), the optimal observation times for each group are marginally later than those corresponding to Scenario 2 (uninformative prior distribution). This is perhaps due to the increased confidence in the dose-response relationship, meaning that we can confidently wait longer without the potential for all chickens in a group to appear infectious following a single (or few) transmission event(s) (i.e., if the dose corresponds to a very high probability of infection).

The designs obtained under the MAPE utility are interesting. Under an informative prior distribution, targeting only the dose-response parameters results in a similar design to that obtained under the EKLD – five groups with observation times of roughly 1.5 (marginally after the mean time to pass through the latent-period), and doses allocated near to the ID_{50} . However, once consideration is also given to the transmission rate parameter, β , the optimal designs are those that allocate all chickens to only two groups, with lower doses (i.e., less initially exposed chickens), and later observation times (i.e., allow more transmission events to occur).

Under an uninformative prior distribution, the optimal design corresponding to only the dose-response parameters is to allocate all individuals to only two groups at the middle of the doses which could correspond to the ID_{50} (see Figure S1b). However, once again, considering the transmission parameter β changes the optimal designs. In particular, consideration of *only* the transmission parameter corresponds to low dose and late observation time – similar to under the informative prior distribution – however, when considering both the dose-response parameters and transmission rate parameter, the optimal design allocates five groups amongst these two distinct regions. Moreover, the second group is allocated between targeting the transmission rate parameter (small dose, late observation time), and the dose-response parameters (higher dose, earlier observation time) – highlighting the obvious trade-off between better estimation of the dose-response parameters, or the transmission parameter.

In each case, it appears as though the designs found using the MAPE utility out-perform the corresponding designs under the EKLD utility. The bias in each parameter estimate is not considerably different under the different designs (EKLD vs. MAPE). As the simulation studies are conducted using parameters sampled from the prior distribution, it is not unexpected that each posterior distribution is centred on the correct value on average, as a random sample from the prior distribution would also achieve this. Where we can observe a difference in the bias between the designs resulting from the two different utilities is when we have uninformative prior distributions. In particular, the MAPE designs appear to have a smaller bias, on average, for the dose-response parameter α , when the designs were evaluated to target (α, δ) , or (α, δ, β) , and for β when the designs were evaluated to target (α, δ, β) or (β) (Figure S6).

Figures S5 and S7 demonstrate the reduction in variance for each parameter, having conducted the experiment under each of the different optimal designs, compared to the variances of the prior distribution. Again, it appears as though the MAPE designs outperform the EKLD designs – that is, the posterior distributions have smaller variance, on average. In fact, the posterior variance under the EKLD designs is marginally worse than that of the prior distribution – suggesting that this allocation of resources provides no further information about the system than was achievable under the prior distribution. The only instance that the EKLD designs out-perform

the MAPE designs appear to be with regards to the dose-response parameter α . Under the informative prior distributions, the posterior variance of α is worse under the MAPE design than the corresponding EKLD design, once consideration is also given to the transmission rate parameter β (i.e., considering (α, δ, β) or (β)). Note also that in the case where (α, δ, β) are being considered, the less-improved variance for α is made up by considerably reduced variance for β , compared to the EKLD design. Under the uninformative prior distributions, the EKLD design only appears to outperform the MAPE design with respect to the posterior variance of α when considering *only* β – that is, when not considering α at all. This appears reasonable, as the MAPE design is clearly targeting only those parameters of interest, and thus loses accuracy about α in order to improve accuracy about the other parameters. Conversely, the posterior variances evaluated at the EKLD designs do not appear to change considerably when targeting different parameter combinations. Thus, if only a subset of the model parameters are of interest, it appears as though these can be more accurately targeted using the MAPE utility, rather than the EKLD utility.

References

- [1] S. B. Duffull, G. Graham, K. Mengersen, and J. Eccleston. Evaluation of the pre-posterior distribution of optimized sampling times for the design of pharmacokinetic studies. *Journal of Biopharmaceutical Statistics*, 22:16–29, 2012.
- [2] J. M. McGree, C. C. Drovandi, and A. N. Pettitt. A sequential Monte Carlo approach to derive sampling times and windows for population pharmacokinetic studies. *Journal of Pharmacokinetics and Pharmacodynamics*, 39:519–526, 2012.
- [3] D. J. Price, N. G. Bean, J. V. Ross, and J. Tuke. An Induced Natural Selection Heuristic for Evaluating Bayesian Optimal Experimental Designs. *arXiv preprint*, 2017. URL <https://arxiv.org/abs/1703.05511>.

4. Appendix

4.1. Results: INSH Algorithm

Figures S8 and S9 shows the progression of the INSH algorithm towards regions of the design space of high-utility, for each of the four scenarios for both the EKL and (negative) MAPE.

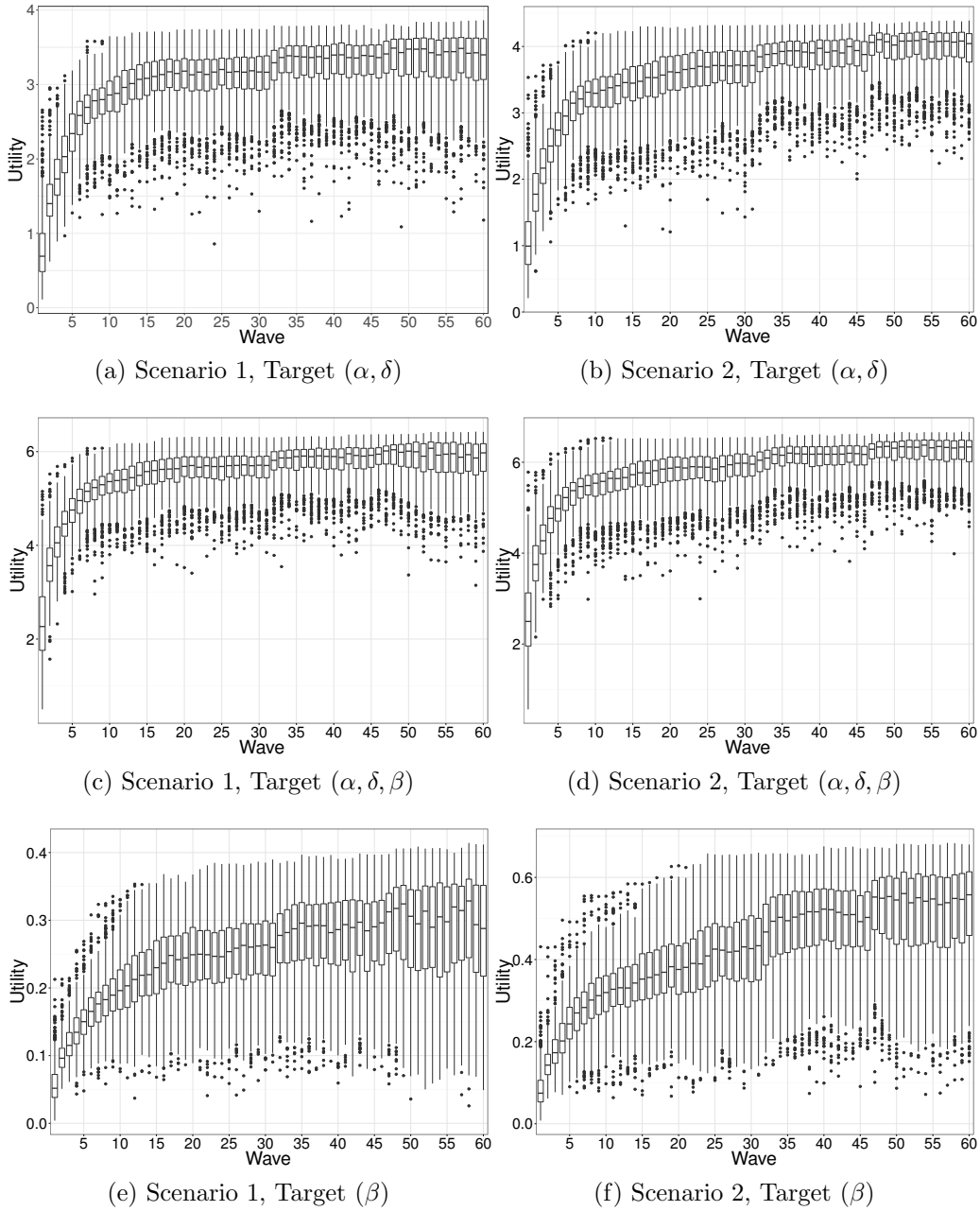


Figure S8: Estimated utility (EKLD) of designs considered at each wave of the INSH algorithm, for Scenarios 1 and 2, when targeting each of (α, δ) , (α, δ, β) , and β , respectively.

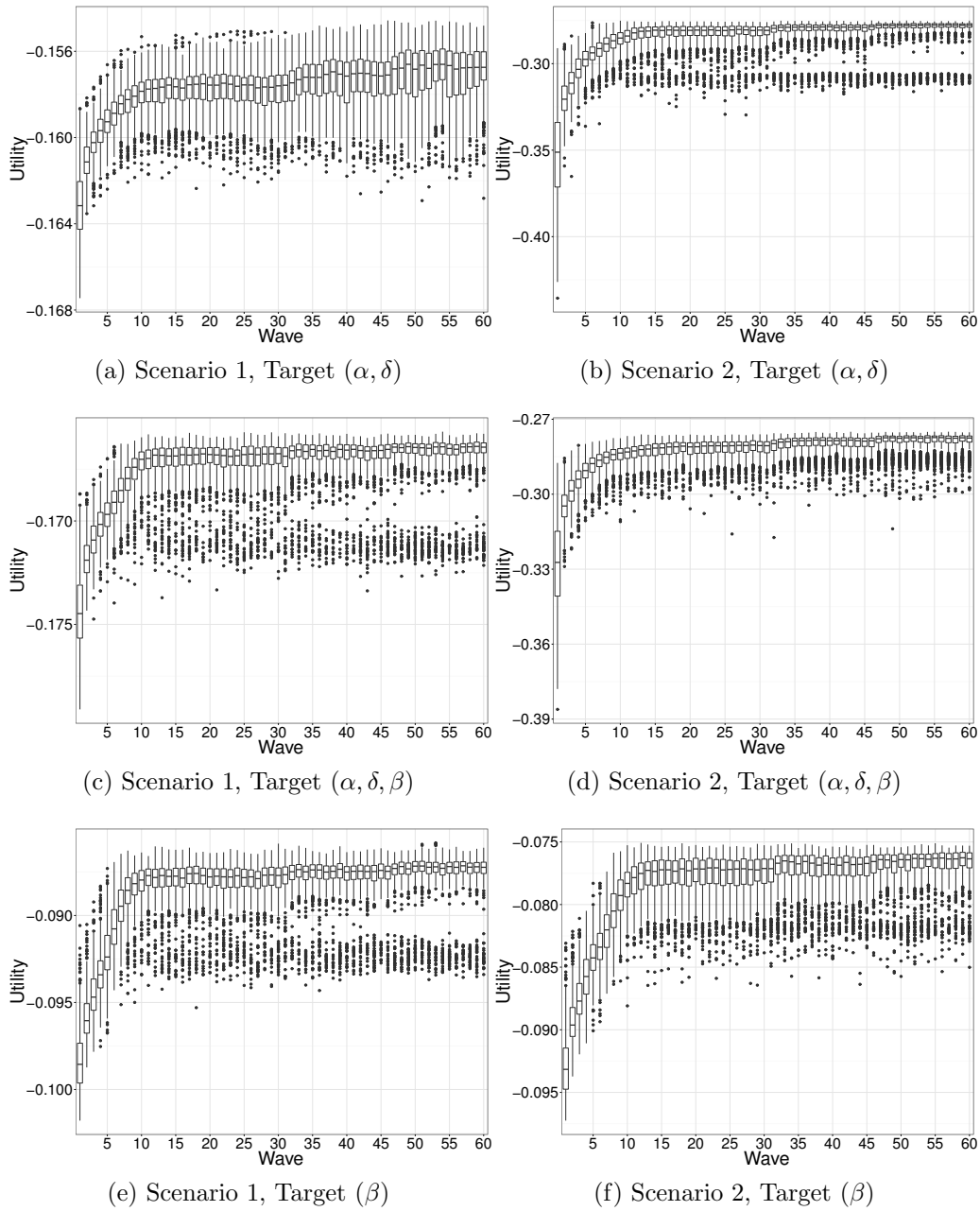


Figure S9: Estimated utility (MAPE) of designs considered at each wave of the INSH algorithm, for Scenarios 1 and 2, when targeting each of (α, δ) , (α, δ, β) , and β , respectively.

Figures S10 and S11 show the proportion of the total designs considered that are made up of each of $G = 2, 3, 4, 5$ groups, across each wave of the INSH algorithm.

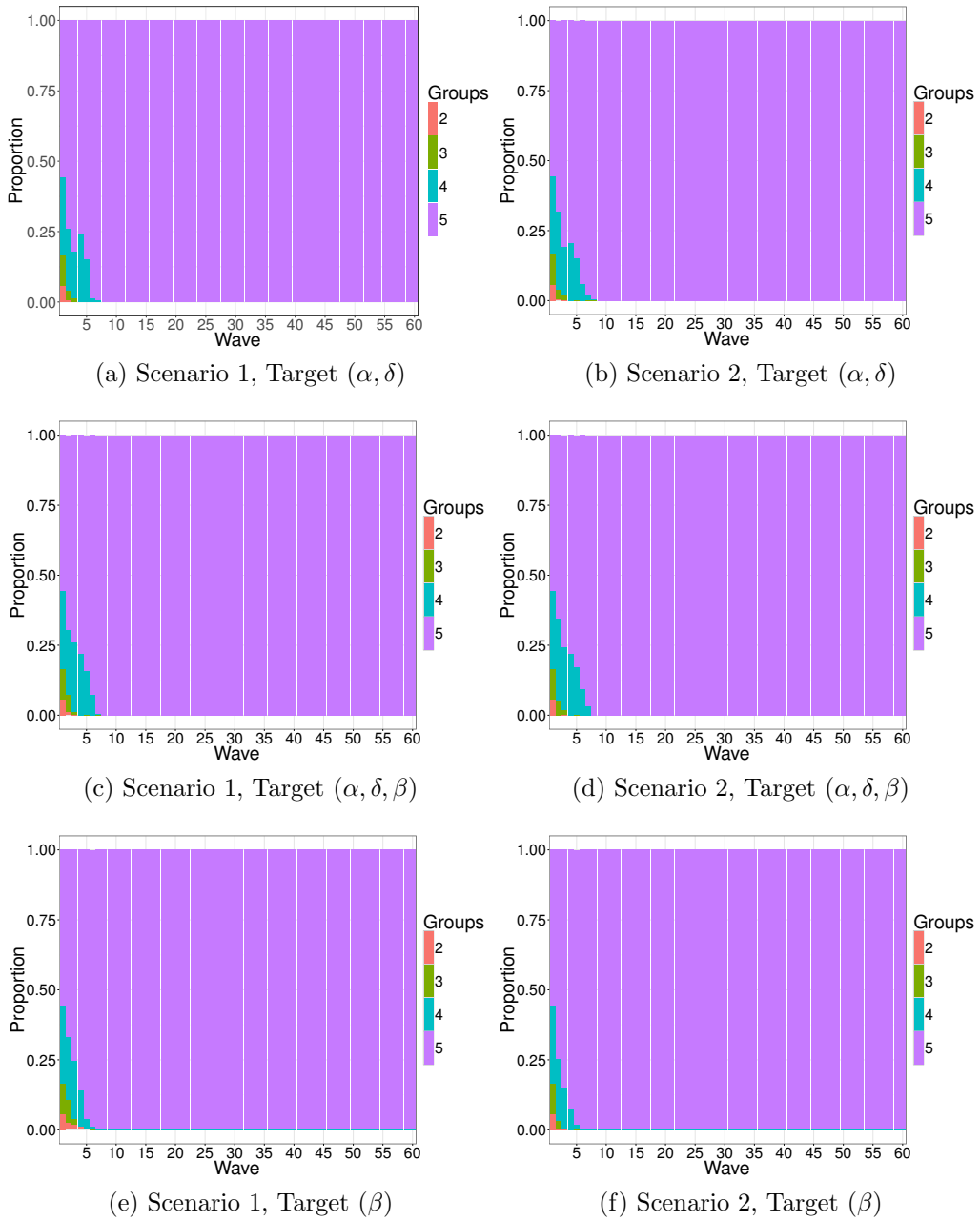


Figure S10: Proportion of the designs being considered at each wave of the INSH algorithm (EKLD), coloured by how many groups in each design, for Scenarios 1 and 2, when targeting each of (α, δ) , (α, δ, β) , and β , respectively.

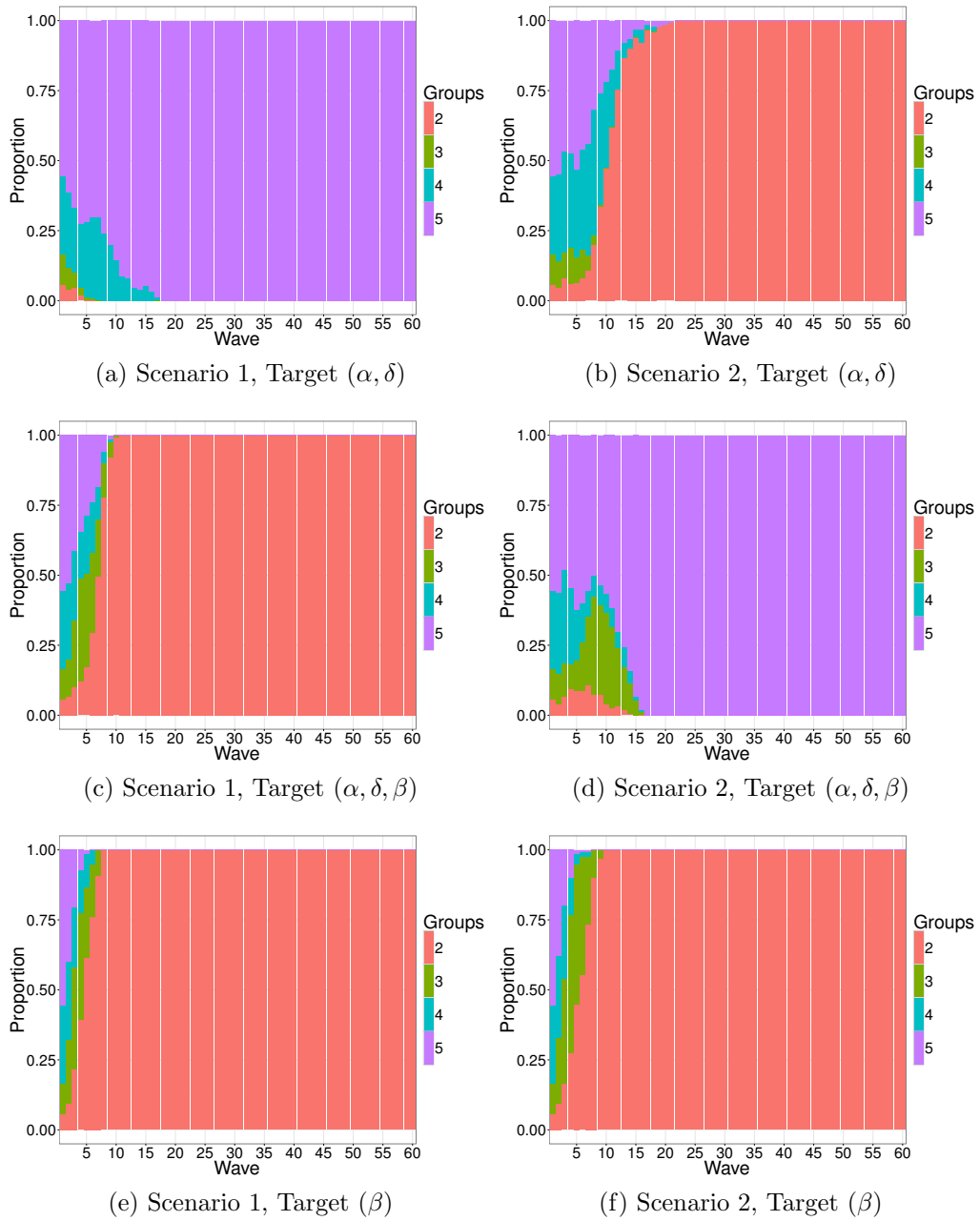


Figure S11: Proportion of the designs being considered at each wave of the INSH algorithm (MAPE), coloured by how many groups in each design, for Scenarios 1 and 2, when targeting each of (α, δ) , (α, δ, β) , and β , respectively.